Cell. Mol. Life Sci. (2012) 69:1331–1352
DOI 10.1007/s00018-011-0879-z

Cellular and Molecular Life Sciences

RESEARCH ARTICLE

Functional mechanisms of the cellular prion protein (PrP^C) associated anti-HIV-1 properties

Sandrine Alais · Ricardo Soto-Rifo · Vincent Balter · Henri Gruffat · Evelyne Manet · Laurent Schaeffer · Jean Luc Darlix · Andrea Cimarelli · Graça Raposo · Théophile Ohlmann · Pascal Leblanc

Received: 20 June 2011 / Revised: 15 October 2011 / Accepted: 24 October 2011 / Published online: 11 November 2011

Abstract The cellular prion protein PrP^C/CD230 is a GPI-anchor protein highly expressed in cells from the nervous and immune systems and well conserved among vertebrates. In the last decade, several studies suggested that PrP^C displays antiviral properties by restricting the replication of different viruses, and in particular retroviruses such as murine leukemia virus (MuLV) and the human immunodeficiency virus type 1 (HIV-1). In this context, we previously showed that PrP^C displays important similarities with the HIV-1 nucleocapsid protein and found that PrP^C expression in a human cell line strongly reduced HIV-1 expression and virus production. Using different PrP^C mutants, we report here that the anti-HIV-1 properties are mostly associated with the amino-terminal 24-KRPKP-28 basic domain. In agreement with its reported RNA chaperone activity, we found that PrP^C binds to the viral genomic RNA of HIV-1 and negatively affects its translation. Using a combination of biochemical and cell imaging strategies, we found that PrP^C colocalizes with the virus assembly machinery at the plasma membrane and at the virological synapse in infected T cells. Depletion of PrP^C in infected T cells and microglial cells favors HIV-1 replication, confirming its negative impact on the HIV-1 life cycle.

Keywords Prion · PrP^C · HIV-1 · Restriction factor · Anti-viral · RNA · Translation

Electronic supplementary material The online version of this article (doi:10.1007/s00018-011-0879-z) contains supplementary material, which is available to authorized users.

S. Alais · R. Soto-Rifo · V. Balter · H. Gruffat · E. Manet · L. Schaeffer · J. L. Darlix · A. Cimarelli · T. Ohlmann · P. Leblanc
Université de Lyon, 69000 Lyon, France

S. Alais · R. Soto-Rifo · H. Gruffat · E. Manet · J. L. Darlix · A. Cimarelli · T. Ohlmann · P. Leblanc
Human virology department, INSERM U758, 69007 Lyon, France

S. Alais · R. Soto-Rifo · V. Balter · H. Gruffat · E. Manet · L. Schaeffer · J. L. Darlix · A. Cimarelli · T. Ohlmann · P. Leblanc
Ecole Normale Supérieure de Lyon, 69007 Lyon, France

V. Balter
CNRS UMR 5276 "Laboratoire de Géologie de Lyon", Lyon, France

L. Schaeffer · P. Leblanc (✉)
Laboratoire de Biologie Moléculaire de la Cellule (LBMC) UMR5239 CNRS/ENS/Université de Lyon/HCL, Ecole Normale Supérieure de Lyon, 69007 Lyon, France
e-mail: Pascal.Leblanc@ens-lyon.fr

G. Raposo
Structure and Membrane Compartments and PICT-IBiSA, Institut Curie, CNRS-UMR144, 12 Rue Lhomond, 75005 Paris, France

Abbreviations

HIV	Human immunodeficiency virus
GPI	Glycosyl phosphatidyl inositol
DRMs	Detergent-resistant microdomains
TEMs	Tetraspanin-enriched microdomains
TNTs	Tuneling nanotubes
UTR	Untranslated region
GFP	Green fluorescent protein
OR	Octa repeat
HC	Hydrophobic core
TM	Transmembrane
PLAP	Placental alkaline phosphatase
VSVg	Vesicular stomatitis virus glycoprotein

LVs	Lentivectors
ELISA	Enzyme-linked immunosorbent assay
KD	Knock down
FACS	Fluorescent activated cell sorter
WT	Wild type
RT	Reverse transcriptase
FL	Full length

Introduction

The cellular prion protein PrP^C/CD230 is a glycosylphosphatidylinositol (GPI) anchor protein strongly conserved among species and is predominantly expressed at the plasma membrane (PM) in various tissues and cells of the nervous and lymphoreticular systems. At the PM, PrP^C is mostly associated with detergent-resistant microdomains (DRMs/Rafts; for review [1]) and in erythroblasts, PrP^C is associated with tetraspanin-enriched microdomains (TEMs) [2]. Interestingly, PrP^C was found to directly interact with tetraspanin-7 (CD231/TALLA-1), suggesting that TEMs could play a role in PrP^C cellular trafficking [3]. The bad reputation acquired by PrP^C originates from its association with transmissible spongiform encephalopathies, a group of fatal neurodegenerative disorders affecting both humans and animals [4]. However, despite these negative connotations, this small protein turns out to be involved in many important biological processes [1]. It has been suggested that PrP^C is involved in cell death and survival, autophagy, processing of sensory information, embryogenesis, hematopoetic stem cell renewal, cell proliferation and differentiation, cell adhesion and migration, and most recently in cytoskeleton dynamics as demonstrated by its capacity to modulate the formation of filopodia, tunneling nanotubes (TNTs) and lamellipodia [1, 5–9]. The analysis of the distribution of PrP^C in T-lymphocytes revealed that it coimmunoprecipitates with Grb2, Fyn kinase, p56Lck and ZAP-70 proteins, as well as with the gangliosides GM1 and GM3 found at the immunological synapse [10–12]. Interestingly, cross-linking of plasma membrane associated PrP^C with an anti-PrP^C mAb revealed strong activation of Fyn in neuronal cells [13] together with MAP kinase phosphorylation and an elevation of intracellular calcium concentration in T-lymphocytes, confirming its implication in signaling pathways and T-cell activation (for review [1, 6]).

PrP^C was also found to be involved in oxidative stress, suggesting that it could belong to a family of factors responding to cell injury [1, 6]. Bacterial and viral infections are major stresses that cells must actively counteract to survive. For this purpose, cells have elaborated defense systems consisting of host factors able to specifically block pathogens replication. Host restriction factors (HRFs), such as TRIM5α, the cytidine deaminase APOBEC 3G or the GPI-anchored protein Tetherin/BST2/CD317, have been characterized in the past decade as potential antiviral factors blocking retroviruses such as HIV-1 at the early or late steps of replication [14]. Interestingly, in the past few years, many studies have revealed a close relationship between the expression of PrP^C and viral replication. In most cases, PrP^C expression has been shown to inhibit replication of various viruses, suggesting that PrP^C could participate in a viral host cell defense pathway. Indeed, Coxsackievirus B3 replication was shown to be more efficient in cells derived from the $PrP^{-/-}$ mouse brain [15]. Recently, the Zinkernagel group observed that activation of an endogenous murine retrovirus (IMERV-1) in the germinal centers of mouse spleens following viral immune stimulation leads to upregulation of PrP^C and an associated specific inhibition of IMERV-1 replication [16]. Similar data indicated that overexpression of PrP^C can affect murine leukemia virus production [17]. Interestingly, PrP^C has also been found to restrict adenovirus 5 replication in HuH7 cells [18]. Analyses of PrP^C expression revealed that PrP^C mRNA expression was upregulated in human primary astrocytes infected by HIV-1 [19] or in human hepatocytes infected by HCV [20], suggesting that PrP^C upregulation could correspond to a cellular response against infection. More recently, PrP^C protein expression was also found to be upregulated in neurons from HIV-1-infected patients presenting neurocognitive disorders [21]. We previously showed that human PrP^C is a nucleic acid chaperone protein that mimics the HIV-1 nucleocapsid protein NCp7 in vitro. NCp7 is a viral protein essential for HIV-1 assembly and replication that plays a key role as an RNA chaperone and is involved in several aspects of the viral RNA biology (incorporation into virions, reverse transcription, etc.) [22–24]. Interestingly, we also reported that HIV-1 virus production and infectivity are strongly reduced upon coexpression of PrP^C 293T cells [25] and that PrP^C is recruited into HIV-1 virions [26]. Taken together, these data prompted us to characterize the antiviral properties of PrP^C in more detail by specifically focusing our study on the cellular and molecular mechanisms by which PrP^C negatively affects HIV-1 replication.

Here, we report that PrP^C expression strongly decreases HIV-1 expression and virus production. We present evidence that these properties are specified by the N-terminal 23–145 region of PrP^C and more specifically to a basic amino acid-rich domain 24-KRPKP-28 within this region. We also show that PrP^C binds to the viral genomic RNA and reduces the translation rate, thus explaining the decrease in expression of Gag and the strong reduction in virus production. Using biochemical and immunofluorescence techniques, we found

that PrP^C can colocalize with HIV-1 Gag as well as Env at the sites of budding in HIV-1-infected T cells, more specifically at the virological synapse. In agreement with these results, we found that PrP^C is released in large quantities into the extracellular medium in association with HIV-1 viral particles. Using specific PrP^C knockdowns, we demonstrate that PrP^C silencing enhances viral replication in HIV-1 target cells.

Materials and methods

Cell lines

The 293T human embryonic kidney cell line was obtained from Généthon (Evry, France), the human U251-MG glioblastoma cells was a gift from Jonas Fuxe, and the microglial cell line was kindly provided by Marc Tardieu and Olivier Rohr. HeLa P4 cells (provided by Olivier Schwartz, Institut Pasteur) are CD4+ and express Lac-Z gene under the control of the HIV-1 LTR. HIV-1-infected cells turn blue after X-Gal staining. These cells were cultured in Dulbecco's modified Eagle's medium (DMEM) supplemented with 10% (v/v) fetal calf serum (FCS), L-glutamine and penicillin/streptomycin. CEM-GFP, established by Jacques Corbeil, is a T-lymphocytic cell line that expresses the green fluorescent protein (GFP) under the control of the HIV-1 LTR. These cells were cultured in RPMI medium (Invitrogen) supplemented with 10% FCS, L-glutamine and penicillin/streptomycin.

Human primary monocytes were obtained using peripheral blood mononuclear cells from healthy donors at the Etablissement Français du Sang de Lyon. The differentiation of monocytes into immature DCs or macrophages was achieved by culturing for 4 days in granulocyte-macrophage colony-stimulating factor (GMCSF) and interleukin 4 (IL-4) at 100 ng/ml (both from AbCys, Paris, France) or granulocyte-macrophage colony-stimulating factor, respectively. Primary blood lymphocytes (PBLs) were obtained by Ficoll purification. PBLs were stimulated for 24 h with phytohemagglutinin (PHA) (Sigma) and interleukin 2 (IL-2) (AIDS Reagent and Reference Program of the NIH) prior to infection. All cells were maintained in RPMI 1640 medium supplemented with 10% fetal bovine serum (5% for DCs) and with the cytokine used for their differentiation.

Constructs

The HIV-1 DNA pNL43 construct has been previously described [27]. The pNL43-Renilla construct was provided by Théophile Ohlmann. The pAF-huPrP^C, -huPrP^{C}ΔGPI and -PLAP constructs encode the human cellular prion protein PrP^C/CD230, the human PrP^C with the GPI anchor deleted and the placental alkaline phosphatase (PLAP) respectively and have been previously described in [25]. The mutants pAF-huPrP^C (ΔOR, ΔHC/TM, Δ24-28, Δ24-145, Δ36-50 and Δ95-110) were created by PCR mutagenesis. The constructs pcDNA3-moPrPFlag, -moShadooFlag and -moDoppelFlag encoding the murine version of PrP, Shadoo and Doppel respectively together with a flag epitope were kindly provided by David Westaway [28]. The constructs pcDNA3#2124, #2944, #2945, #3099 or #3042, #3043 and #3044 encoding respectively hamster WT PrP and mutants A117V, AV3 and SA-PrP, and the human WT PrP^C and mutants A117V and G114V were kindly provided by Ramanujan Hegde [29, 30].

The pcDNA3moPrPΔ23-31 construct encoding the murine PrP^C with residues 23–31 deleted was kindly provided by David A. Harris.

The pCR3Tetherin-HA construct was kindly provided by Paul Bieniasz [31], and pCMV5UTRGlob-Renilla was provided by Théophile Ohlmann. The pEGFPC1 construct encoding enhanced GFP was from Clontech.

The p8.2 plasmid packaging construct encoding the HIV-1 Gag, GagPol and Tat, Rev, Nef, Vif and Vpr regulatory and accessory proteins and the pVSVg plasmid encoding the vesicular stomatitis envelope glycoprotein (VSVg) were provided by Didier Trono [32]. The HIV-1 lentivector pAPM was a gift from Jeremy Luban [33].

The p8.2, pVSVg and pAPM constructs were used to generate lentiviral vectors encoding mirShRNAs (see RNA lentivector production section).

The cloning of microRNA-based short hairpin RNAs (shRNAs) into the pAPM HIV-1 lentivector specific for human PrP^C was performed in the context of an HIV-1 lentiviral construct that allows their stable expression upon viral transduction (pAPMshRNA). The vector pAPMshRNA contains an expression cassette for puromycin and another for the microRNA-based shRNAs [33].

Primer sequences were designed through the Open Biosystems website facility. Three microRNA-based shRNAs per gene target were simultaneously used to silence human PrP^C. The primers used were as follows: mirShRNA1 (TGCTGTTGACAGTGAGCGAGCATTCCTTTCTTTAAACTATTAGTGAAGCCACAGATGTAATAGTTTAAAGAAAGGAATGCCTGCCTACTGCCTCGGA), mirShRNA2 (TGCTGTTGACAGTGAGCGCGGAGGCCACATGATACTTATTTAGTGAAGCCACAGATGTAAATAAGTATCATGTGGCCTCCTTGCCTACTGCCTCGGA) and mirShRNA3 (TGCTGTTGACAGTGAGCGCGCACTGAATCGTTTCATGTAATAGTGAAGCCACAGATGTATTACATGAAACGATTCAGTGCATGCCTACTGCCTCGGA). We used the pAPMmirShRNA Luciferase as a negative control [33]. The above-mentioned primers were used as a matrix in a PCR reaction with the following forward and reverse primers: miR30-XhoI (5′-GATGGC

TGCTCGAGAAGGTATATTGCTGTTGACAGTGAGCG) and miR30-EcoRI (3′-GTCTAGAGGAATTCCGAGGCAG TAGGCA). The PCR products were then cloned as XhoI/EcoRI fragments directly into the pAPM vector and sequenced.

Transfection and virus production

Co-transfection of 293T cells was performed by the phosphate calcium method in six-well plates (4.5×10^5 cells per well) with 1.2 μg of HIV-1 pNL43 and 1.2 μg of constructs encoding the WT or mutant human, murine or hamster prion proteins. Twenty-four hours after transfection, cells were washed with PBS and incubated for an additional 16 h with complete medium. Cell culture supernatants containing viral particles were harvested 40 h after transfection, clarified and virus production monitored by measuring the reverse transcriptase (RT) activity released.

Preparation of WT HIV-1 virions was performed as follows: 293T cells (3×10^6) were transfected with the pNL43 molecular clone (20 μg) by the calcium phosphate method. Virions were recovered 40–48 h post-transfection, centrifuged at 3,000×*g* for 10 min and filtered through a 0.45-μm-diameter pore filter, aliquoted and stocked at −80°C before a reverse transcriptase activity determination or ELISA CAp24 assay was made [25].

Lentivector production and RNA interference

Lentivectors (LVs) were produced by calcium phosphate DNA transfection of 293T cells with the HIV-1 packaging construct p8.2, a miniviral genome bearing the expression cassette encoding the mirShRNA-Lu/PrP under the H1 promoter and the plasmid encoding the VSVg envelope. For vector production, packaging, transfer and envelope-encoding plasmids were transfected at a ratio of 8:8:4 μg for 3×10^6 cells plated 1 day before transfection in 100-mm dishes. LVs were purified from the supernatant of transfected cells by ultracentrifugation through a 25% (wt/vol) sucrose cushion or used directly. Viral particles (mirSHRNA-Lu and mirSHRNA-PrP) were then resuspended in 1× PBS, aliquoted, frozen at −80°C and normalized by an exogenous reverse transcriptase assay. Transductions of CEM-GFP cells were carried out in the presence of 8 μg/ml of polybrene for 2 h. One day after transduction, cells were cultured for 4 days in the presence of puromycin (0.7 μg/ml) until the death of non-transduced control cells was complete. Efficiency of the knock-down was monitored by Western blotting using an anti-PrP antibody. Alternatively, improved knock down was realized by making a double transduction of CEM-GFP cells. Briefly, cells were transduced a first time, selected with puromycin and transduced a second time and let under puromycin selection until infection with WT-HIV-1.

Cell proliferation

Puromycin-selected cells (KD-Lu and KD-PrP) were cultured in 24-well plates and counted each day for 1 week.

HIV-1-infected cells

CEM-GFP cells were infected with HIV-1 virions (50 ng CAp24) for 5 h in complete culture medium and were analyzed between 4 to 6 days after infection until they reached the level of 40–60% GFP-positive cells as measured by FACS analysis. Activated PBLs were infected in similar conditions in parallel with CEM-GFP cells using the same dilutions as that of the HIV-1 virions.

For kinetic experiments, the first set of experiments was carried out using 5×10^4 cells (CEM-GFP or microglial cells KD-Lu or KD-PrtP) infected with HIV-1 WT (200 ng of CAp24/1 $\times 10^6$ cells) in 24-well plates during a period of 7–9 days in a 400-μl final volume; 50 μl of cell supernatants was collected each day and replaced with 50 μl of fresh medium. At the end of the kinetic analyses, reverse transcriptase activity was monitored as previously described [34]. Alternatively, double-transduced KD-Lu and KD-PrP^C CEM-GFP cell lines were cultured in 12-well plates and infected with WT-HIV-1 with 80 ng of CAp24/1 $\times 10^6$ cells for low MOI and 400 ng of CAp24/1 $\times 10^6$ cells for high MOI. Cells and cell culture supernatants were recovered each day during 6 days. Cell culture medium was monitored for RT activity and virus infectivity released.

Western blotting

The Western blotting procedures were as previously described [25].

Immunofluorescence and confocal microscopy imaging

293T HIV-1/PrP^C and HIV-1/mutant-PrPs coexpressing cells or U251-MG, monocyte-derived dendritic and macrophage cells were grown on 12-mm-diameter coverslips in six-well plates. Immunofluorescence (IF) staining was performed at room temperature. The cells were washed with PBS, fixed with 2% paraformaldehyde in 1× PBS for 15 min, quenched with 50 mM NH4Cl, permeabilized by 0.1% Triton X-100 for 5 min and blocked 1 h in 1× PBS in 1% BSA. The fixed cells were labeled for 1 h with the primary antibody mix (anti-PrP^C, anti-MAp17 and anti-Envgp120) in 1% bovine serum albumin-PBS, washed and stained for 45 min with the corresponding fluorescent secondary antibody in 1% bovine serum albumin-PBS

(see supplementary Materials and Methods for primary and secondary antibody specificities). The cells were then washed several times with 1× PBS and mounted on microscope slides with antifading immunomount (CML Immunomount) prior to image acquisition. For non-adherent cell lines (CEM, CEM-SS, Jurkat and CEM-GFP) and primary cells (monocytes and PBLs) uninfected or infected by HIV-1, cells were washed in clean culture medium and centrifuged at 1,000 rpm to eliminate dead cells and cellular debris. Then 2×10^4 cells were loaded on SuperFrostRPlus microscope slides and incubated for 15 min at room temperature in a humidified chamber. Adherent cells were then fixed in 2% PFA and handled as described above for immunofluorescence analyses.

Images were acquired using the Spectral Confocal Microscope (TCS SP5 AOBS, PLATIM platform ENS Lyon) with Argon 488/458, HeNe 543, HeNe 633 lasers and Plan Apochromat 63 × 1.4 oil objective, supplied with LSM 510 3.4 software. Co-localization between Gag, Env, Vpu, Nef and PrP^C was determined using ImageJ Software.

Cell-cell contacts, virological synapses and nanotubes

HIV-1-infected CEM-GFP cells (5×10^5 cells) were mixed with activated PBLs (5×10^5 cells) and put in contact at 37°C on $SuperFrost^R$Plus microscope slides during 3 h in a humidified chamber. Adherent cells were then fixed with 2% PFA at RT and immunofluorescence carried out as previously described.

Immunoprecipitation and RT-PCR analyses

293T cells (3×10^6) were cotransfected by the calcium phosphate method with 10 µg of pNL43 and 10 µg of $pAHHuPrP^C$. Then 48 h after transfection, cells were resuspended in PBS, pelleted and lysed in IP buffer [1% NP40, 50 mM Tris pH 8.0, 150 mM NaCl supplemented with protease inhibitor cocktail (Complete Roche) at 4°C during 30 min]. Immunoprecipitation of PrP was performed with the PrP monoclonal antibody SAF32 or with mouse IgG as a control antibody on 400 µg of post-nuclear supernatant for 2 h at 4°C. Protein G magnetic beads (Dynal) were added and incubated for another 2 h at 4°C. The beads were then pelleted and washed 3× with IP buffer. One third of the beads were used for Western blotting analysis using the SAF32 antibody and soluble protein A/G peroxidase (Pierce). The remaining 2/3 was used for RNA extraction. The beads were proteinase K treated (15 min at 55°C) in the presence of SDS and RNase inhibitor. RNAs were extracted using the TRIzol® Reagent (Invitrogen Co.) and precipitated using RNAse-free glycogen and isopropanol. The RNA pellet was resuspended in RNase-free water and treated with RQ1 DNAse 1 h at 37°C. RNAs were then phenol chloroform extracted and precipitated as described above. Purified RNAs were resuspended in RNase-free water and used for cDNA synthesis using reverse transcriptase superscript II (Invitrogen) with random hexamer oligonucleotides as primers (Invitrogen). As positive controls, cDNAs were also synthesized from cellular RNAs of 293T cells expressing HIV-1 pNL43. Once obtained, cDNAs were used as a template for PCR reactions to amplify the unspliced HIV-1 genomic RNA using the sense and antisense oligonucleotides (CTA GGGAACCCACTGCTTAAGCCT position 502–525 in pNL43) and (CAAGCAGCAGCTGACACAGGA position 1138–1158), respectively, producing a specific 657-bp PCR fragment. Controls for the RT-PCR included the exclusion of RT and the use of mouse IgG immunoprecipitates.

HIV translation analysis

Renilla activity

Briefly, 4.5×10^5 293T cells were cotransfected with 1.2 µg of $pAFHuPrP^C$-FL or $pAFHuPrP^C$-Δ24-28 with 1.2 µg of HIV-1 pNL43-Renilla or pCMV5UTRGlob-Renilla. The medium was replaced with fresh medium 24 h after transfection. Then 40 h after transfection cells were recovered and Renilla activity monitored using the Renilla Luciferase Assay System (Promega Co., Madison, WI, USA) in a Veritas Luminometer (TurnerBiosystems).

RNA extraction and RT-qPCR

RNA extraction and RT-qPCR were performed as previously described [35]. Briefly, 293T cells cotransfected with Renilla-based DNAs (pNL43-renilla or pCMV5UTRGlob-Renilla) and PrP constructs ($pAFHuPrP^C$-FL or the deleted mutant Δ24-28) or the pEGFPC1 construct as negative control were washed four times with PBS and lysed with 200 µl of RLNa buffer [10 mM Tris-HCl (pH 8.0), 10 mM NaCl, 3 mM MgCl2, 1 mM DTT, 0.5% NP40 and 15 U/ml of RNaseOUT (Invitrogen Co.)]. Whole cell extracts were centrifuged at 13,000 rpm for 4 min to pellet nuclei and obtain the cytoplasmic fraction. For total RNAs cytoplasmic fractions were recovered and RNA extraction carried out by adding 1.25 ml of TRIzol® reagent (Invitrogen Co.) as recommended by the manufacturer. Extracted cytoplasmic RNAs (200 ng) were reverse-transcribed using the qScript™ Flex cDNA kit (Quanta Biosciences). For quantitative PCR, a 20-µl reaction mix was prepared with 5 µl of template cDNAs (previously diluted to 1/10), 10 µl of MESA green SYBR premix (Eurogentec), 0.2 µM of sense and antisense primers and subjected to amplification using a fluorescence thermocycler (Applied Biosystems 7000

Real-time PCR, Foster City, CA). The housekeeping gene GAPDH was amplified in parallel to serve as a control reference. Relative copy numbers of Renilla luciferase cDNAs were compared to GAPDH using x-DCt (where x corresponds to the experimentally calculated amplification efficiency of each primer couple).

Results

PrP^C and Shadoo affect HIV-1 expression and production while Doppel has no effect

We previously found that PrP^C expression reduces expression of both wild-type HIV-1 Pr55Gag and viral particles, while PrP^C deleted for the GPI anchor domain has little or no effect, suggesting that trafficking of PrP^C is crucial for these effects [25]. As a control, PLAP, a well-characterized raft-associated GPI-anchored protein, only moderately affected HIV-1 viral production, confirming that the negative effect of PrP^C was specific and not due to the overexpression of a GPI-anchored protein [25].

Because PrP^C is highly conserved across mammals, we evaluated whether murine PrP^C ($moPrP^C$) could also affect HIV-1 expression and viral production. For this purpose 293T cells were cotransfected with a WT infectious HIV-1 molecular clone and constructs encoding $huPrP^C$-WT, $huPrP^C$-ΔGPI, PLAP or murine PrP^C ($moPrP^C$). Virus production was assessed 2 days after transfection by measuring the reverse transcriptase (RT) activity released into the cell culture medium. Similar results were obtained using ELISA CAp24 determination assay (see Fig. S1A). As expected, we confirmed the effects of $huPrP^C$-WT, $huPrP^C$-ΔGPI and PLAP, and found that $moPrP^C$ displays a similar effect as that of $huPrP^C$ (Fig. 1b) decreasing Gag expression (Fig. 1c) and virus production (Fig. 1b), and indicating that anti-HIV properties of PrP^C are conserved across species. Similar data were also obtained with hamster PrP^C (Fig. S2B).

Two paralogs of PrP^C, termed Doppel (Dpl) and Shadoo (Sho), have been characterized and found to be functionally connected to PrP^C biology and associated neurological disorders [36, 37]. Dpl and Sho are small GPI-anchored proteins that share structural similarities with PrP^C. Doppel is a divergent homolog of PrP^C that only shares conservation with PrP^C at its C-terminal globular domain, while Shadoo is highly homologous to the N-terminal part of PrP^C (Fig. 1a). This led us to hypothesize that one of the two paralogs could potentially possess anti-HIV-1 properties similar to those of PrP^C. We thus tested the influences of Dpl and Sho expression on HIV-1 Pr55Gag expression and viral particle production. The results presented in Fig. 1b, c indicate that although Dpl does not impact on Pr55Gag expression and virus production, Sho reduces both in a similar manner to PrP^C (compare Pr55Gag in lanes 1, 2 with lanes 3, 5 and also 7, Fig. 1c). These data thus suggest that the anti-HIV-1 properties can potentially be associated with the N-terminal region of PrP^C. Interestingly, we found previously that the PrP^C 23–145 region has nucleic acid chaperone activities similar to those of the HIV-1 nucleocapsid protein NCp7 [22, 23]. For these reasons, we then focused our attention on the 23–145 region of PrP^C and set out to characterize domains potentially associated with antiviral properties.

The unstructured amino terminal domain of PrP^C possesses anti-HIV-1 properties

To further characterize the domain(s) associated with the antiviral properties of PrP^C, a series of deletions encompassing amino acids 23–145 of PrP^C were generated (Fig. 2a) and tested as above. The data presented in Fig. 2b indicate that the mutant with a deletion of amino acids 24–145 has no significant effect on Pr55Gag expression (compare lanes 6 and 2 with the control lane 1) and only moderately reduced viral particle production (see Fig. 2b), confirming that this region carries most of the anti-HIV-1 determinants. To better characterize these determinants, we deleted several domains that could potentially be associated with the nucleic acid chaperone activity. Deletion of the octarepeat region (PrP-ΔOR) affected HIV-1 virus production with a similar efficiency to that of the full length PrP^C (12–16-fold), suggesting that the OR domain does not carry anti-HIV-1 activity (Fig. 2b). Because basic amino acid residues are often associated with nucleic acid binding and nucleic acid chaperone activity, this prompted us to focus our attention on basic domains distributed within the 23–145 region. Three major regions containing basic residues were identified. The first one is located at positions 23–28, downstream of the SP sequence, the second at position 36–50 and the last at position 95–110 (Fig. 2a). Deletion mutants were generated and for each tested in cotransfection assays with the WT HIV-1 construct. The data presented in Fig. 2b indicate that the PrP-Δ36-50 affects HIV-1 virus production with an efficiency similar to WT-PrP^C, suggesting that these residues are not essential for the antiviral activity. Interestingly, the mutant with residues 95–110 deleted reduced the virus production an additional threefold compared to PrP^C, suggesting that these residues can modulate the antiviral properties of PrP^C. On the other hand, we found that the mutant with the five basic residues 24-KRPKP-28 deleted moderately affected Pr55Gag expression and virus production, suggesting that this small basic domain plays an essential role in the anti-HIV-1 properties. Similar data were obtained using a murine version of this mutant (moPrP-Δ23-31; data

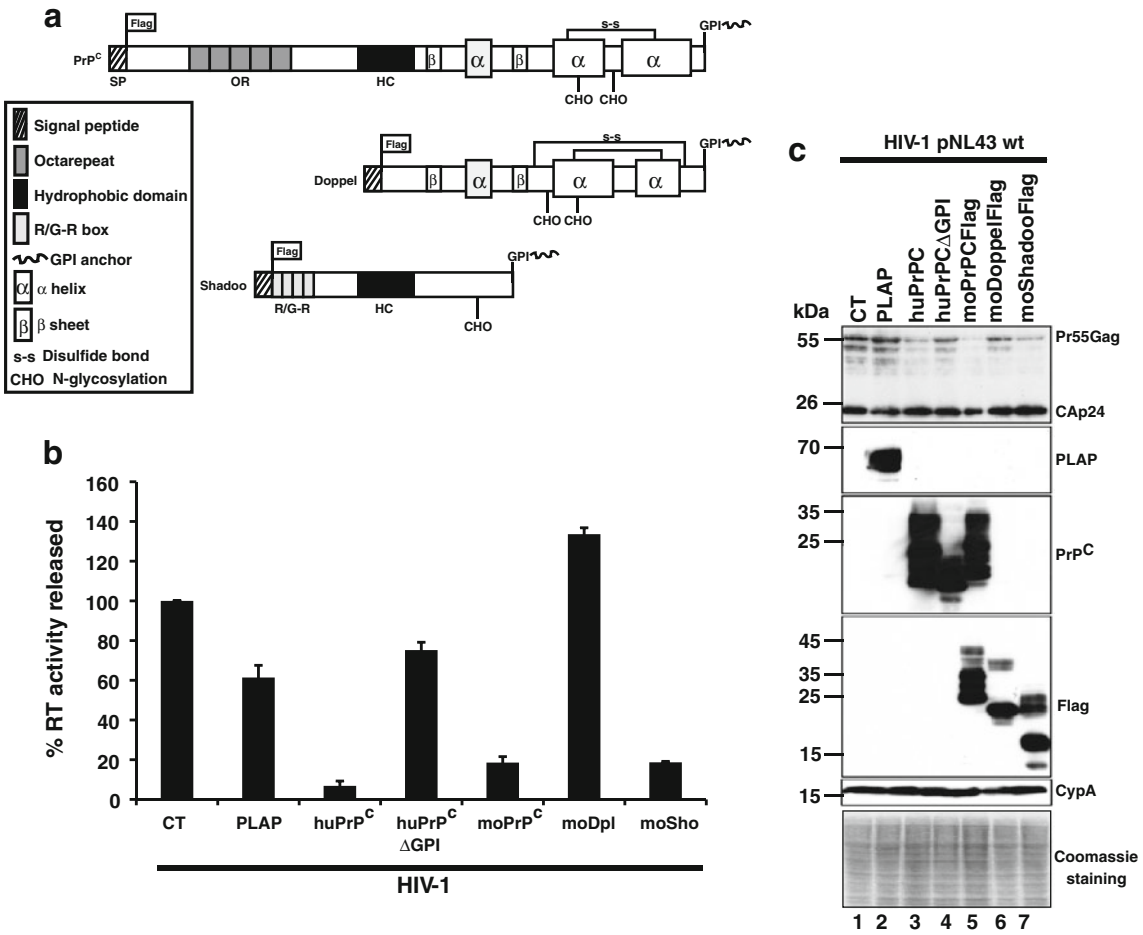

Fig. 1 PrP^C and Shadoo, but not Doppel, affect HIV-1 expression and production. **a** Schematic representation of the PrP^C, Doppel and Shadoo GPI anchor proteins. **b** Viral supernatants from HIV-1/Control (CT)/PLAP (placental alkaline phosphatase)/human huPrP^C and /huPrP^{C}ΔGPI or /murine moPrP^C,/moDoppel and/moShadoo co-transfected cells were harvested 48 h after transfection and the virus-associated reverse transcriptase (RT) activity measured. Data shown are representative of three independent experiments. Values are given as means ± SD. **c** Virus-producer cells were analyzed by Western blotting. Total protein (10 µg per lane) of HIV-1/CT (*lane 1*); HIV-1/PLAP (*lane 2*); HIV-1/WT-PrP^C (*lane 3*); HIV-1/PrP^{C}ΔGPI (*lane 4*); HIV-1/moPrP^C (*lane 5*); HIV-1/moDoppel (*lane 6*); HIV-1/moShadoo (*lane 7*) was analyzed by SDS PAGE. Membranes were probed with antibodies directed against HIV-1 CAp24, PLAP, PrP^C, Flag tag for PrP^C and moDoppel, moShadoo. Cyclophilin A (CypA) and coomassie staining were used as loading controls

not shown), confirming that this small basic domain is also essential in the murine version of PrP^C.

Recent studies identified the cellular GPI-anchored protein Tetherin/CD317/BST-2 as a potential restriction factor inhibiting HIV-1 viral production, most prominantly HIV-1 ΔVpu, by tethering the viral particles at the cell surface [31, 38]. The host restriction factor Tetherin is anchored to the plasma membrane (PM) via its GPI moiety and crosses the PM via a transmembrane domain located in its amino terminal region. Interestingly, PrP^C displays a similar topology mediated by a hydrophobic core/transmembrane domain (HC/TM; position 111–129) located in the amino-terminal part of the protein downstream of the octarepeat region (position 53–90). The HC/TM domain is involved in the formation of the so-called ^{CTM}PrP transmembrane topological isoform [39], which resembles the topology of the Tetherin restriction factor [40]. The presence of the TM in Tetherin is essential for its antiviral function, and its deletion completely abolishes the restriction activity [41]. Interestingly, deletion of the Tetherin GPI anchor also completely destroys its antiviral properties [41]. Since we found that the GPI-deleted PrP^C mutant has only a minor effect (1.8-fold decrease; [25]) on HIV-1 Pr55Gag expression and virus production (Fig. 1b), we investigated whether the antiviral properties of PrP^C could be driven by a ^{CTM}PrP topology. To answer this question, we generated a PrP^C mutant in which the HC/TM domain was deleted, and we tested this mutant as above. Surprisingly, the results indicate that the PrP-ΔHC mutant strongly reduces HIV Pr55Gag expression and decreases viral production over 100-fold (see Fig. 2b, c, lane 4). Similar data were obtained using a deleted mutant in which the HC/TM

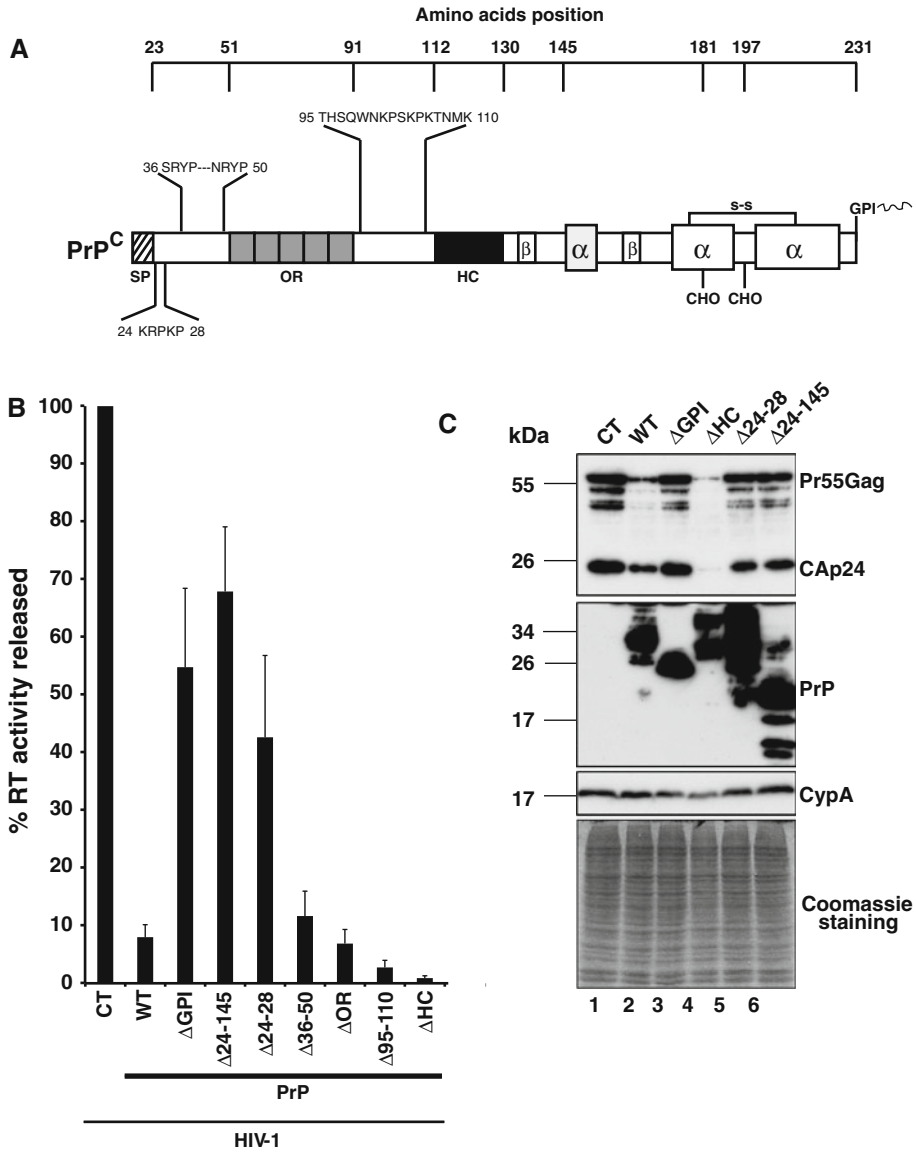

Fig. 2 Anti-viral properties of PrP^C map to the N-terminal region. **a** Schematic representation of PrP^C with amino acid positions and deleted domains. **b** Viral supernatants from 293T cells co-transfected with HIV-1 pNL43 and control vector (CT), full length WT PrP^C (WT), or PrP^C deletion mutants PrP-ΔGPI, Δ24-145, Δ24-28, Δ36-50, ΔOR, Δ95-110 or ΔHC were harvested 48 h after transfection and released virus associated RT activity was measured. Data shown are representative of six independent experiments. Values are given as means ± SD. **c** Virus producer cells were analyzed by Western blotting. Total protein (10 µg per *lane*) of HIV-1/CT (*lane 1*); HIV-1/PrP^C-WT (*lane 2*); HIV-1/PrP-ΔGPI (*lane 3*); HIV-1/PrP-ΔHC (*lane 4*); HIV-1/PrP-Δ24-28 (*lane 5*); HIV-1/PrP-Δ24-145 (*lane 6*) was analyzed by SDS PAGE. Membranes were probed with antibodies directed against HIV-1 CAp24 and PrP^C. Cyclophilin A (CypA) and Coomassie staining were used as loading controls. Note that the Pr55Gag protein level was strongly reduced in PrP^C-WT and ΔHC samples

was replaced by the Flag epitope (data not shown). These data indicate that the anti-HIV-1 properties are not conferred by the ^{CTM}PrP isoform. However, our data suggest that the HC/TM domain can efficiently modulate the antiviral effects of PrP^C. To confirm these data, similar experiments were carried out using the human PrP mutants A117V and G114V that were previously found to favor the formation of the ^{CTM}PrP isoform [29, 30]. The data presented in Fig. S2A indicate that induction of ^{CTM}PrP formation does not potentiate the anti-HIV-1 properties of PrP^C. Similar results were also obtained using the hamster mutants A117V and AV3 that stimulate ^{CTM}PrP isoform formation (Fig. S2B). Using a mutant version of PrP that produces only ^{CTM}PrP isoform (SA-PrP) [29], we confirmed that ^{CTM}PrP does not carry the anti-HIV properties. These data clearly indicate that ^{CTM}PrP is not involved in PrP anti-HIV-1 properties and reveal that PrP^C and Tetherin, despite being two GPI proteins with a similar topology, have a different mode of action on HIV-1.

We next investigated whether infectivity of virions released was affected in the different experimental conditions. For this purpose, HeLa P4 cells (an HIV infection indicator cell line) was infected with RT-normalized virions from the different conditions (Fig. S3A). Virus infectivity was monitored after X-Gal staining by determining the number of infected blue cells (*β*-galactosidase activity measure), and the data indicated that infectivity of HIV-1 virions was decreased when PrP^C-WT and PrP-ΔHC were expressed, whereas it was partially recovered in the PrP-ΔGPI or PrP-Δ24-28 expression context. The decrease of virus infectivity was correlated with a strong decrease of the envelope glycoprotein expression (Fig. S3B), confirming our previously published data [25].

Because PrP^C binds copper efficiently (through the histidine residues contained in the OR domain or those located at residues 96, 111 and 187 [1]) and copper has long been shown to possess biocidal properties against bacteria, fungi and a variety of enveloped and non-enveloped viruses, we decided to test the copper concentration in the cell supernatant of HIV-1/CT versus HIV-1/PrP^C-WT and mutants (ΔOR, ΔHC and Δ24-28) coexpressing cells using inductively coupled plasma mass spectrometry (ICP-MS). The data presented in Fig. S4 revealed that the copper concentration was slightly increased when PrP^C-WT was expressed. However, the copper concentration decreased to the background with the same efficiency for the PrP-ΔOR, -ΔHC or -Δ24-28 mutants compared to the PrP^C-WT. Since the copper concentration decreased independently of the PrP-mutants (ΔOR, ΔHC and Δ24-28) that affect or not HIV-1 Gag and Env expression and virus production, these data strongly suggest that in our experimental conditions, copper is not a crucial factor for the PrP^C anti-viral properties.

Coexpression of PrP^C and Tetherin strongly affects HIV-1 expression and production

We previously demonstrated that PrP^C and Tetherin inhibit HIV-1 production by different mechanisms, suggesting that coexpression of the two proteins should strongly inhibit HIV-1 expression and production. To investigate this possibility, PrP^C and Tetherin were coexpressed in the presence of WT HIV-1 or a Vpu deleted mutant (ΔVpu). The data presented in Fig. 3 show that PrP^C affects the Pr55Gag expression and virus production of both HIV-1 WT and ΔVpu, whereas Tetherin, as expected, strongly affects the virus production of ΔVpu, but only moderately the release of WT virions [38] (Fig. 3a). Conversely to PrP^C, Tetherin blocks HIV-1 release without affecting Gag expression, confirming previously published data (compare lanes 3 and 7 with lanes 1 and 5 in Fig. 3b, [31, 38]). Interestingly, the effect of PrP^C was stronger on HIV-1 WT production compared to Tetherin, but similar effects were observed with ΔVpu (Fig. 3a). When PrP^C and Tetherin

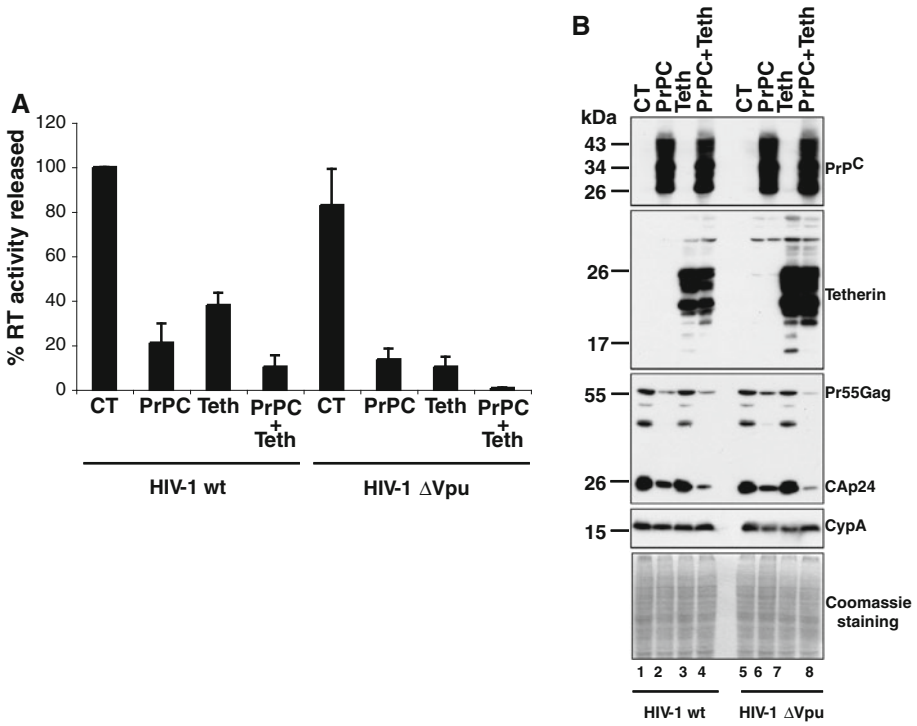

Fig. 3 PrP^C and Tetherin affect HIV-1 in a different manner. **a** Viral supernatants from 293T cells coexpressing HIV-1 pNL43 (WT or ΔVpu mutant) and PrP^C-WT or Tetherin-HA or PrP^C-WT +Tetherin-HA were recovered 40 h after transfection, and virus-associated RT activity was monitored. Data shown are representative of three independent experiments. Values are given as means ± SD. Note the strong effect on HIV-1 virus production of PrP^C and Tetherin when they were coexpressed compared to PrP^C or Tetherin alone. **b** Virus producer cells were analyzed by Western blotting. Total protein (10 μg per *lane*) of HIV-1WT/CT (*lane 1*); HIV-1WT/WT-PrP^C (*lane 2*); HIV-1 WT/Tetherin-HA (*lane 3*); HIV-1 WT/WT-PrP^C + Tetherin-HA (*lane 4*) and the same but with the HIV-1Δvpu mutant (*lanes 5–8*) was analyzed by SDS-PAGE. After transfer, membranes were probed with antibodies directed against HIV-1 CAp24, PrP^C and HA epitope for Tetherin-HA fusion protein. Cyclophilin A (CypA) antibody and Coomassie staining were used as loading controls. Note that the Pr55Gag protein level was strongly reduced in PrP^C-FL and Tetherin coexpressing cells

were coexpressed, we observed a strong additive and negative effect on both HIV-1 Pr55Gag expression and virus production, reaching a final 200-fold reduction in the case of the ΔVpu virus (Fig. 3a, b lanes 4 and 8). These data thus indicate that coexpression of host factors with antiviral properties can be a potential way for infected cells to efficiently block HIV-1 replication.

PrP^C is expressed in HIV-1 target cells

To determine whether the anti-HIV-1 properties of PrP^C can also be observed in a more relevant cell system, the expression of PrP^C was monitored in different HIV-1 target cells (Fig. 4a), such as T lymphoblastic cell lines (CEM-GFP, lane 1) and primary cells such as peripheral blood cells (monocytes, lane 2; monocyte-derived dendritic cells—MDDCs, lane 3; activated peripheral blood lymphocytes—PBL, lane 4; monocyte-derived macrophages—MDM, lane 5). All cells tested expressed variable amounts of PrP^C with different levels of glycosylation (non, mono- and di-glycosylated isoforms), suggesting that PrP^C could have different functions depending on the cell type. In the course of this study, we found that the T lymphoblastic cell line CEM-GFP presented similar levels of expression and glycosylation as compared to activated PBLs (compare lane 1 with lane 4), suggesting that this cell line could be an interesting cellular model.

Analysis of PrP^C cellular distribution by immunofluorescence using an anti-PrP^C antibody (Fig. 4b) indicated that PrP^C is predominantly distributed both at the plasma membrane and in filopodial protrusions in the glioblastoma adherent cell line U251-MG (see white arrowheads in panel 1). In T cells and PBLs (panels 2 and 5, respectively), PrP^C staining was also observed at the PM and in membrane structures resembling filopodial bridges and/or tunneling nanotubes (TNTs, see white arrowheads in

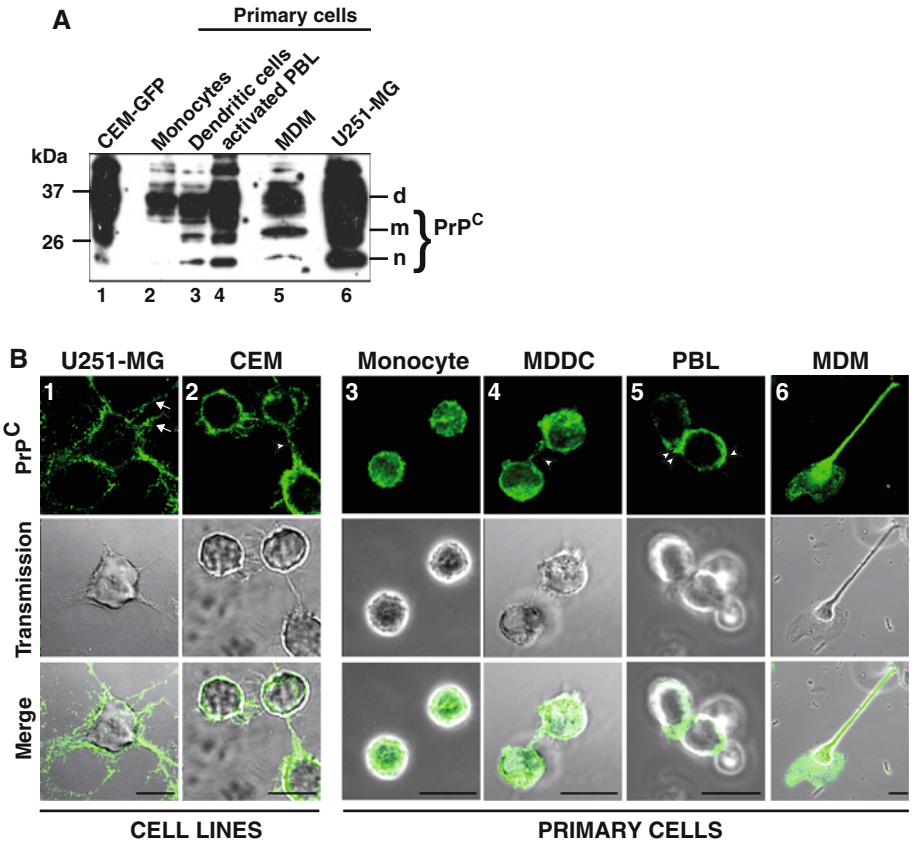

Fig. 4 PrP^C is expressed in HIV-1 target cells. **a** Western blotting analysis of PrP^C expressing cells; 10 µg of total protein extracts of cell lines or peripheral blood mononuclear cells was analyzed by SDS-PAGE, and transferred membranes were probed with the monoclonal SAF32 anti-PrP. *Lane 1* lymphoblastoid cell line CEM-GFP; *lane 2* monocytes; *lane 3* monocyte-derived dendritic cells (MDDC); *lane 4* activated peripheral blood lymphocytes (PBLs); *lane 5* monocyte-derived macrophages (MDM); *lane 6* the glioblastoma cell line U251MG. **b** Distribution of PrP^C by confocal immunofluorescence in U251MG cells (*panel 1*); CEM lymphoblastoid cells (*panel 2*); primary monocytes (*panel 3*); monocyte-derived dendritic cells (MDDC, *panel 4*); PBLs, *panel 5*; monocyte-derived macrophages (MDM, *panel 6*). Note the presence of PrP^C signal (*green*) at the plasma membrane, in filopodia (see *white arrows* for U251MG cells), in tunneling nanotubes (see *white arrowheads* in CEM and MDDC) and at the immunological synapse (see double *white arrowheads* for activated PBL). *Scale bars* are 10 µm

panels 2 and 4) as previously reported [8, 42]. Similar data were obtained with the MDDC and MDM cells (see panels 4 and 6, respectively). In activated PBL preparations, the PrP^C signal was strongly enhanced at the immunological synapse (IS) (see white arrowheads in panel 5), confirming previous findings on T-cell and dendritic cell synapses [43]. Monocytes were for the most part isolated and expressed PrP^C both at the cell surface and also intracellularly (panel 3). As expected, intracellular PrP^C was also detected in all the cells tested, emphasizing the trafficking of PrP^C between the cytosol and the PM.

PrP^C colocalizes with Gag and Env in HIV-1-infected T lymphocytes

We previously found that PrP^C cofractionated with HIV-1 Gag and Env in the DRMs/raft microdomains of 293T PrP^C/HIV-1 coexpressing cells [25]. Similar data were observed with HIV-1-infected CEM-GFP cells (data not shown), strongly suggesting that PrP^C could be located at the site of HIV-1 assembly and budding in infected T cells. To determine if PrP^C colocalizes with HIV-1 Gag and Env in infected CEM-GFP T cells, immunofluorescence experiments were performed using antibodies directed against PrP^C, HIV-1 Gag and Envgp120. The data presented in Fig. 5a show that PrP^C (panel 2) colocalizes with HIV-1 Env (panel 3) and Gag (panel 4) in specific plasma membrane domains in a polarized fashion (panel 5). A perfect colocalization of PrP^C with the HIV-1 Nef and Vpu accessory proteins was also observed, confirming that PrP^C is distributed at the site of assembly and budding (data not shown). Interestingly, immunofluorescence experiments performed on HIV-1-infected PBLs revealed a similar colocalization among PrP^C, Gag and Env (Fig. S5A), further validating the CEM/CEM-GFP cell line as a good cellular model to study PrP^C-HIV-1 interplay. Crosslinking with an anti-PrP antibody, SAF32, showed that PrP^C and Gag cocluster in the same membrane microdomain (Fig. S5B) confirming again that PrP^C and Gag colocalize in the same membrane microdomain.

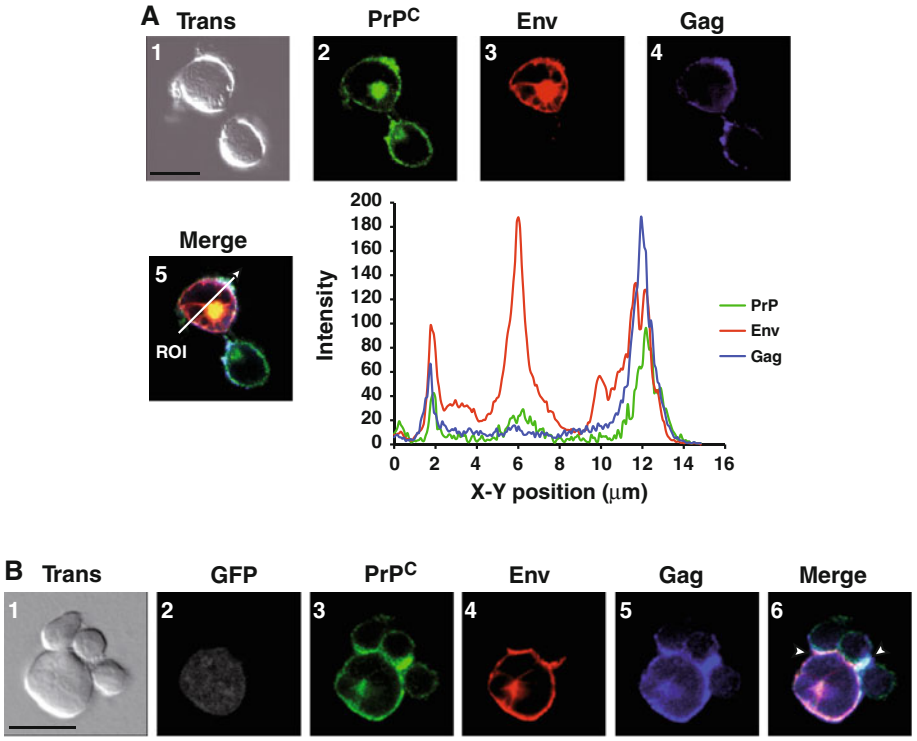

Fig. 5 PrP^C colocalizes with HIV-1 Gag and Env in infected T lymphocytes. **a** CEM cells infected with HIV-1 were recovered 5 days after infection, fixed and analyzed by confocal immunofluoresence using anti-PrP (*panel 2*, *green*), anti-Envgp120 (*panel 3*, *red*) and anti-MAp17 (*panel 4*, *blue*) antibodies. Images are single sections through the middle of the cell with the corresponding transmission image (*panel 1*): areas of *green/red/blue* colocalization appear *white* (*panel 5*). Region of interest (ROI; *white arrow*) is depicted in the merge panel (*panel 5*). The plot profile of PrP^C (*green*)/Env (*red*) and Gag (*blue*) colocalization along the ROI was constructed and analyzed using Image J software. **b** HIV-1 infected CEM-GFP cells were put in contact with activated PBLs for 3 h at 37°C on SuperFrost^{R}Plus microscope slides in an humidified chamber and then fixed. Images are single sections through the middle of the cell with the corresponding Nomarski image (*panel 1*). Confocal immunofluorescence was carried out using anti-PrP (*panel 3*, *green*), anti-Envgp120 (*panel 4*, *red*) and anti-MAp17 (*panel 5*, *blue*) antibodies. *Panel 2* corresponds to GFP fluorescence (grey staining) indicating the HIV-1 CEM-GFP-positive cell. Areas of PrP (*green*)/Env (*red*)/Gag (*blue*) colocalization appear *white* (see *arrowheads* in merge, *panel 6*). Note the strong signal of PrP^C at the virological synapse. *Scale bars* are 10 μm

Recent studies have indicated that intercellular transmission of HIV-1 occurs predominantly by cell–cell contact and especially through a virus-mediated modified immunological synapse called the virological synapse (VS) [44, 45]. Interestingly, the data presented in Fig. 4 (panel 5) suggest that PrP^C is located at the immunological synapse, confirming previously published data [43]. This prompted us to examine whether PrP^C could be recruited to the VS in infected T cells. For this purpose, HIV-1-infected CEM-GFP cells (Fig. 5b panel 2) were put into contact with activated PBLs (see experimental procedures). Cell complexes (panel 1) were fixed and analyzed by immunofluorescence using antibodies directed against PrP^C (panel 3), HIV-1 Envgp120 (panel 4) and Pr55Gag/MAp17 (panel 5). The colocalization of PrP^C with Gag and Env strongly suggests that PrP^C accumulates at the virological synapse (see arrowheads panel 6). These data thus clearly indicate that PrP^C is recruited at the site of HIV-1 assembly and budding in T cells and is enriched where HIV-1 intercellular transmission occurs. These data prompted us to determine if PrP^C could be associated with released HIV-1 viral particles. The data presented in Fig. S6 showed that HIV-1 infection strongly enhances the release of PrP^C into the cell culture medium (Fig. S6A). Furthermore, using sucrose density and optiprep velocity gradients, we also confirmed that PrP^C is physically associated with released HIV-1 viral particles from infected CEM-GFP cells (Fig. S6B, C, D), confirming our previously published data using 293T cells [26].

Knock-down of PrP^C enhances HIV-1 replication in its target cells

We previously found that strong expression of PrP^C negatively affects HIV Gag expression and viral particle production in 293T cells. Interestingly, in the course of the present study, we repeatedly observed an inverse correlation between PrP^C expression (see arrowhead Fig. 6a) and that of Gag and Env in HIV-1-infected CEM-GFP cells (Fig. 6a). Specifically, cells that expressed a low level of PrP^C expressed high levels of HIV-1 Gag and Env (see arrows) and vice versa, suggesting PrP^C negatively influenced HIV-1 expression in infected CEM-GFP cells. Similar data were also observed with infected PBLs (data not shown).

To determine if high expression of PrP^C in CEM-GFP cells can negatively influence HIV-1 replication, PrP^C expression in CEM-GFP cells was downregulated using an HIV-1-derived vector bearing puromycin and a microRNA-based shRNA hairpin expression cassette [33]. Three shRNAs directed against the prion mRNA 3′ untranslated region were selected. A negative control, miR30-ShRNA-Lu, was directed against the *luciferase* gene. HIV-1 vectors containing the three miR30-ShRNA-PrPC or the miR30-ShRNA-Lu control were used to transduce CEM-GFP cells (Fig. 6b, c). After cell transduction and puromycin selection, PrP^C expression was monitored by Western blotting or FACS analyses (Fig. 6b). The data presented in Fig. 6b show that miR30-ShRNA-PrP^C downregulates PrP^C expression, whereas the miR30-ShRNA-Lu control has no effect. The FACS analysis of puromycin-selected cells revealed, despite a high transduction efficiency, that silencing of PrP^C was not absolute

Fig. 6 Knock-down of PrP^C affects HIV-1 replication in T cells. ▶ **a** T-lymphocytes with strong PrP^C expression have reduced expression of HIV-1 Env and Gag. CEM-GFP cells (*panel 1*, transmission) infected with HIV-1 (*panel 2*, GFP expression *grey*) were recovered 5 days after infection, fixed and analyzed by confocal immunofluorescence using anti-PrP (*panel 3*, *green*), anti-Envgp120 (*panel 4*, *red*) and anti-MAp17 (*panel 5*, *blue*) antibodies. Images are single sections through the middle of the cell. Note that cells with high PrP^C expression (*arrowhead*) display low expression of HIV-1 Gag and Env, whereas cells with low PrP^C expression (*arrow*) have high HIV-1 Gag and Env expression. *Scale bars* are 10 µm. **b** CEM-GFP cells were transduced with lentiviral vectors expressing small hairpin RNAs (ShRNAs) surrounded by miR30 sequences directed against the *prnp* gene (miRShRNAs-PrP^C) or the *luciferase* gene (negative control; miRShRNAs-Lu). After puromycin selection, transduced cells [knock-down (KD) Lu and PrP^C CEM-GFP cells] were analyzed by Western blotting (15 µg of protein extracts) using anti-PrP or anti-cyclophilin A (CypA; loading and expression control) or by FACS analyses. *Solid green lines* PrP^C expression in KD-Lu cells. *Solid red lines* PrP^C expression in KD-PrP^C cells. *Dotted green and red lines* negative control KD-Lu and KD-PrP^C cells. Note that silencing of PrP^C is not absolute. **c** Kinetics of HIV-1 infection in KD-Lu or KD-PrP^C CEM-GFP cells. KD-Lu and KD-PrP^C CEM-GFP cells were infected with WT HIV-1, cell culture supernatants were recovered each day for 9 days, and released reverse transcriptase (RT) activity was monitored. *Dotted black lines* RT activity released by HIV-1-infected KD-Lu cells. *Solid black lines* RT activity released by HIV-1-infected KD-PrP^C cells. Note that HIV-1 replication is enhanced in KD-PrP^C cells. **d** Second silencing strategy. CEM-GFP cells were first transduced as previously described above, selected and/or transduced a second time with the same vectors. Three days after transduction, cells were analyzed by Western blotting using anti-PrP antibodies. Loading control was monitored by Coomassie gel staining. S is simple-transduction and D is double transduction. *Lanes 1, 2* correspond to KD-Lu cells and *lanes 3, 4* to KD-PrP cells. **e** Kinetics of HIV-1 infection in double-transduced KD-Lu or KD-PrP^C CEM-GFP cells. Double-transduced KD-Lu and KD-PrP^C CEM-GFP cells were infected with WT HIV-1, at low MOI (80 ng CAp24/1 $\times$ 10^6 cells) or high MOI (400 ng CAp24/1 $\times$ 10^6 cells). Cells and cell culture supernatants were recovered each day for 6 days and released reverse transcriptase (RT) activity monitored. *Dotted black lines* RT activity released by HIV-1-infected KD-Lu cells. *Solid black lines* RT activity released by HIV-1-infected KD-PrP^C cells. Note that HIV-1 replication is twofold enhanced in KD-PrP^C cells at low MOI. **f** Virus infectivity. Virions released at days 4 and 5 (low MOI) were standardized for their RT activity and used for infection of HeLa P4 indicator cell line (CD4+ LTR-LacZ+). Infected cells were revealed by in situ staining for β-galactosidase activity (blue cells) 40 h post infection. Infection was quantified using a β-galactosidase-based colorimetric assay. Note that virions released by KD-PrP^C cells are more infectious compared to virions released by KD-Lu cells

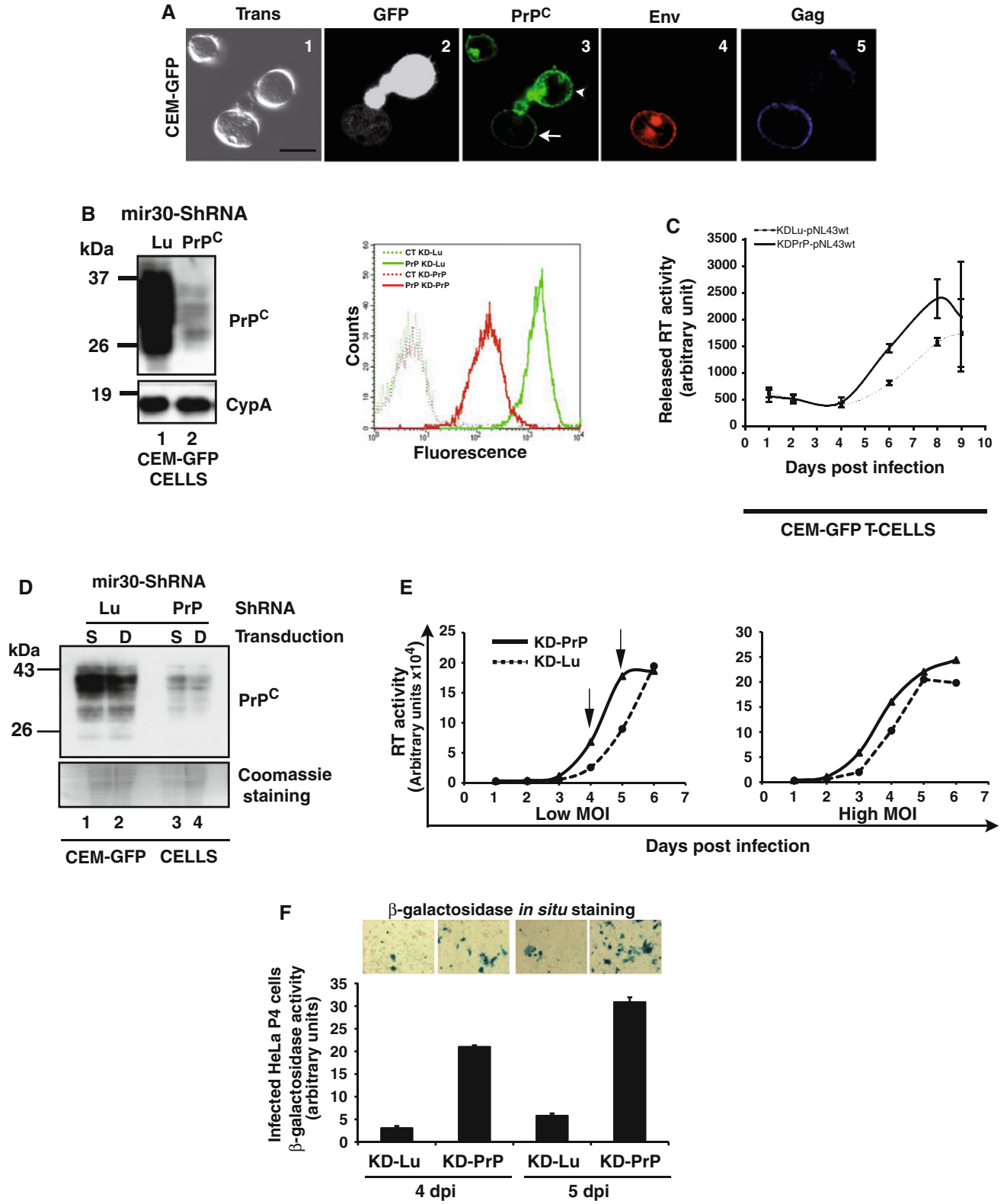

(Fig. 6b). We next investigated the impact of PrP^C silencing on HIV-1 replication in the CEM-GFP cell system. For this purpose, CEM-$GFP^{KD\text{-}Lu}$ and CEM-$GFP^{KD\text{-}PrP}$ cells were infected with WT HIV-1. The supernatants of infected CEM-$GFP^{KD\text{-}Lu}$ and CEM-$GFP^{KD\text{-}PrP}$ cells were recovered and monitored for RT activity for the course of 9 days. Results presented in Fig. 6c indicate that PrP^C silencing significantly enhances HIV-1 replication compared

to the negative control CEM-GFP^{KD-Lu}. To verify that silencing of PrP^C does not affect cell division or the expression levels of HIV-1 CD4 or CXCR4 receptor/coreceptor, puromycin–selected CEM-GFP^{KD-Lu} and CEM-GFP^{KD-PrP} cells were counted for a period of 9 days, during which cell division and CD4/CXCR4 expression were monitored by FACS. The data indicated that cell division, CD4 and CXCR4 expression levels are not affected in the context of PrP^C silencing (data not shown), indicating that the increase of HIV-1 replication observed is specifically linked to PrP^C downregulation. To improve PrP^C KD efficiency, KD-Lu and KD-PrP CEM-GFP cells firstly transduced (S for simple transduction in Fig. 6d lanes 1, 3) were transduced a second time by the respective lentivectors (D for double transduction in Fig. 6d lanes 2, 4). The data presented in Fig. 6D revealed that this new strategy does not really improve PrP^C silencing compared to our previous conditions, suggesting that double knock down is not advantageous here. However, we decided to infect double-transduced cells by the WT-HIV-1 at low or high MOI for 6 days. Infected cell supernatants were recovered each day and monitored for RT activity and virus infectivity released (Fig. 6e, f). The data presented in Fig. 6e confirmed the data previously observed in Fig. 6c with a twofold increase of HIV-1 replication in a low MOI context (Fig. 6e left panel). Analysis of RT activity released in a high MOI context revealed that infection with an increasing amount of HIV-1 virions moderately attenuates the positive effect observed in the low MOI experiment (Fig. 6e right panel). We next analyzed the virus titer at days 4 and 5 post-infection in a low MOI context. For this purpose, virions released were normalized for their RT activity and used to infect HeLa P4 indicator cell line. The data revealed that virions released by KD-PrP^C cells were more infectious (5–7-fold more) compared to virions released by KD-Lu negative control cells (Fig. 6f) confirming the data observed in the 293T cellular system (Fig. S3A). Similar experiments were carried out on virions released by KD-Lu and KD-PrP^C cells from the high MOI infection. The data revealed that virions released by KD-PrP^C cells were only twofold more infectious compared to those released by KD-Lu cells (data not shown).

The central nervous system (CNS) is the major site where PrP^C expression occurs. High PrP^C expression was detected in various CNS cells such as neurons, astrocytes or microglial cells. Microglial cells correspond to the resident macrophages and are the main targets of HIV-1 in the brain. Using a human microglial cell line, we investigated the influence of PrP^C silencing on HIV-1 replication. The data presented in Fig. S7 indicate that PrP^C silencing enhances HIV-1 replication in a similar way to that in infected KD-CEM-GFP cells, thus again confirming the inhibitory effect of PrP^C on HIV-1 replication.

Fig. 7 PrP^C binds to HIV-1 genomic RNA and affects its translation. **a** Immunoprecipitation of PrP^C in 293T HIV-1/PrP^C coexpressing cells (*lane 1*). Coimmunoprecipitations were carried out using the specific monoclonal SAF32 anti-PrP (*lane 3*) or the mouse-IgG as a control antibody (*lane 2*). PrP^C immunoprecipitation was performed by Western blotting using the anti-PrP antibody. Note the strong signal for the PrP immunoprecipitate (*lane 3*), whereas no signal was detected in the mouse IgG control (*lane 2*). **b** Coimmunoprecipitated RNAs associated with anti-PrP (*lanes 5 and 6*) or mouse IgG control antibodies (*lanes 3 and 4*) were extracted and DNAse treated. Purified RNAs were then used for cDNA synthesis in the presence or absence of reverse transcriptase (*lanes 4, 6* and *lanes 3, 5*, respectively). PCR amplification was performed using specific HIV-1 primers located in the 5′UTR and in the *gag* gene (see Materials and Methods). Note the specific 657-bp HIV-1 PCR product only detected in the anti-PrP immunoprecipitates (*lane 6*). Positive RT-PCR samples were carried out with 293T HIV-1/PrP^C cellular RNAs (*lanes 1, 2*). M: DNA molecular weight standards (in bp). **c** Schematic representation of the HIV-1 pNL43-renilla molecular clone. 293T cells were cotransfected with pNL43-luciferase molecular clone and expression constructs encoding the WT full length FL-PrP^C or the inefficient mutant PrPΔ24-28. Measurement of HIV-1 Gag-luciferase activity and quantification of cytoplasmic HIV-1 luciferase-encoding RNAs by quantitative RT-PCR using GAPDH as an internal control was performed in the context of FL-PrP^C or PrPΔ24-28. Total luciferase activity was measured 40 h post-transfection (*left panel*), and the amount of HIV-1 genomic RNA coding for cytoplasmic luciferase was quantified (*middle panel*). Translational efficiency (*right panel*) was calculated by normalizing the total HIV-1 Gag-luciferase activity by reference to the amount of cytoplasmic HIV-1 luciferase RNA. Note that FL-PrP^C strongly affects HIV-1 translation, whereas no effect was observed with the PrPΔ24-28 mutant. **d** Schematic representation of the intronless luciferase coding vector used in this study (pcDNAGlobinRen) showing positions of the CMV promoter and BGH polyadenylation signal. Total luciferase activity was measured 40 h post-transfection (*left panel*) and the amount of cytoplasmic luciferase-encoding mRNAs was quantified (*middle panel*). Translational efficiency (*right panel*) was calculated by normalizing the total luciferase activity by reference to the amount of cytoplasmic luciferase mRNA. Note that PrP^C has no effect

Taken together these data indicate that PrP^C expression negatively influences HIV-1 replication, suggesting that PrP^C could correspond to a factor that is part of a cellular defense system against viral injury.

PrP^C binds to HIV-1 genomic RNA and affects its translation

The cellular and molecular mechanisms by which PrP^C affects HIV-1 Gag expression and virus production are unknown. Using a pulse-chase experimental strategy we previously found that Gag expression was reduced in 293T PrP^C/HIV-1 coexpressing cells, suggesting to us that PrP^C could inhibit HIV-1 Gag expression by affecting the translation level of the viral genomic RNA [25]. These data prompted us to further investigate how PrP^C could reduce HIV-1 Gag translation. Because previous studies showed that PrP^C is a nucleic acid chaperone protein able to bind in vitro to the highly structured HIV-1 TAR RNA sequence

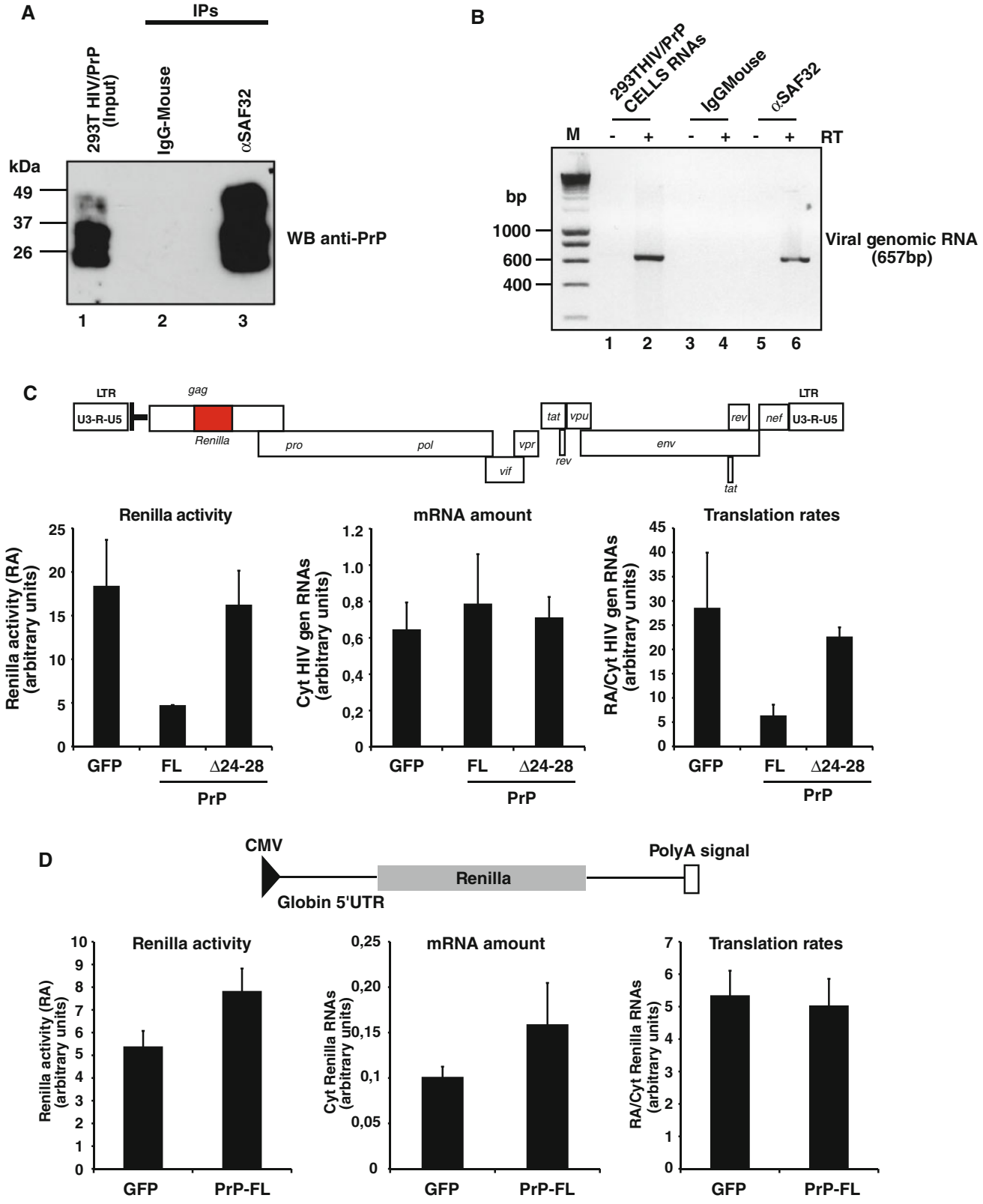

[22, 23], we first tested whether PrP^C could interact with viral genomic RNA in our 293T HIV-1/PrP^C-coexpressing cells. To this end, 293T-HIV-1/PrP^C coexpressing cells (lane 1, Fig. 7a) were lysed and PrP^C was immunoprecipitated using the anti-PrP SAF32 monoclonal antibody (lane 3) or mouse IgG as a negative control (lane 2). A strong

PrP^C immunoprecipitation was observed with the anti-PrP (lane 3), whereas no PrP^C was detected with the control antibody (lane 2). Potential associated RNAs were extracted from the two immunoprecipitates and were analyzed by RT-PCR using oligonucleotides specific for HIV-1 genomic RNA and analyzed by agarose gel. The data presented in Fig. 7b show a 657-bp band corresponding to an HIV-1-specific PCR amplification product (see lanes 2 and 6) from PrP^C immunoprecipitates, whereas no PCR amplification product was detected in the negative mouse IgG control (see lane 4) in the presence or absence of reverse transcriptase (see lanes 1, 3 and 5). These data indicate that HIV-1 genomic RNA is recovered in PrP^C immunoprecipitates and suggest that PrP^C, through this interaction, could repress HIV-1 genomic RNA translation. To shed further light on such an effect, 293T cells were cotransfected with the WT full length FL-PrP^C (or alternatively a construct encoding GFP as a negative control) with a modified version of the WT pNL43 HIV-1 proviral clone containing the renilla luciferase open reading frame inserted within the *gag* gene (see Fig. 7c). As an internal control for PrP^C, we chose to investigate the effect of the previously characterized deletion mutant PrPCΔ24-28. The data presented in Fig. 7c (left panel) show that expression of FL-PrP^C strongly affects the Renilla activity compared to the GFP negative control, whereas the PrPΔ24-28

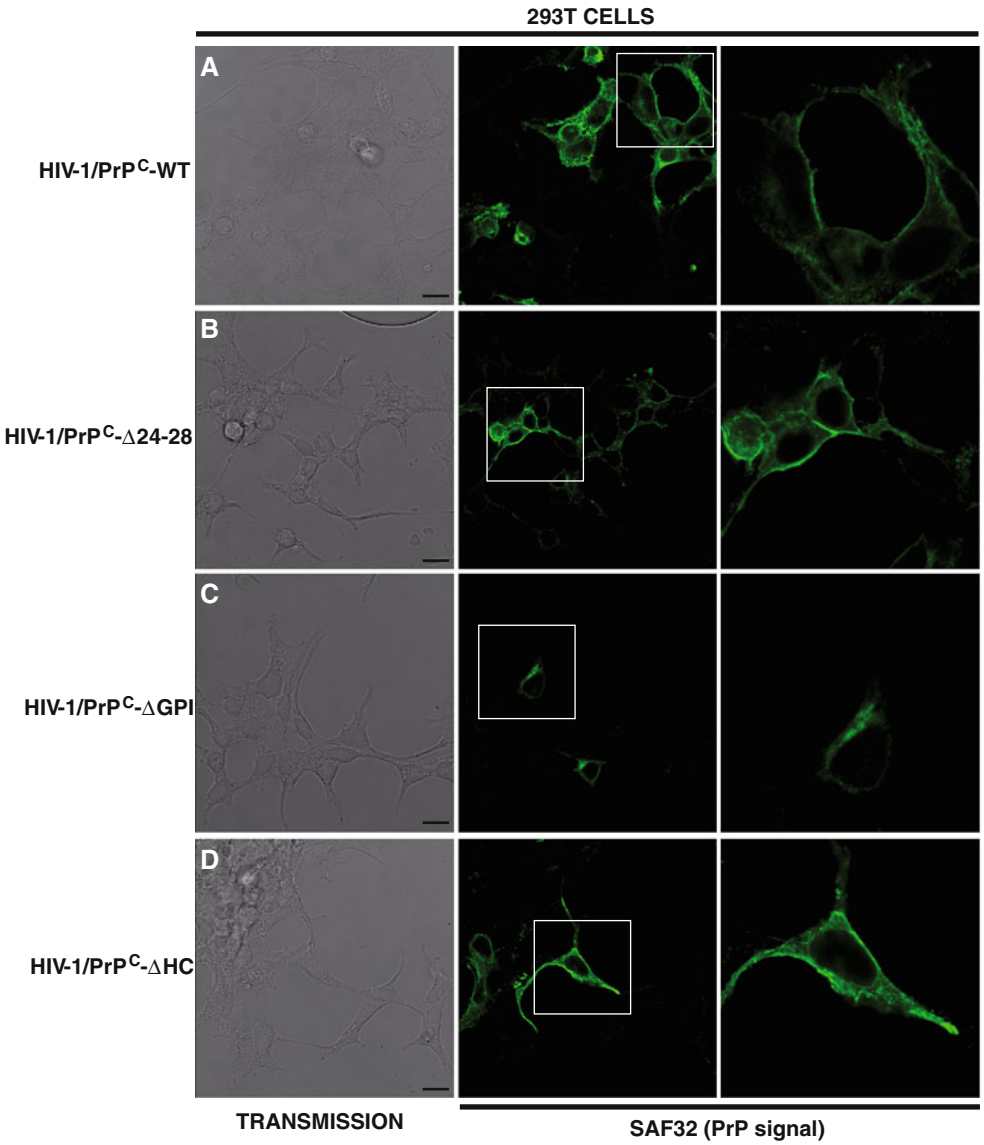

Fig. 8 Cellular distribution of WT and mutant PrPs in 293T HIV-1 coexpressing cells. Cellular distribution of WT and mutant PrPs (WT, Δ24-28, ΔGPI, ΔHC) in 293T coexpressing cells by immunofluorescence using the SAF32 anti-PrP antibody. *Left panel* corresponds to the transmission. *Medium panel* is the PrP labeling for **a** HIV-1/PrP^C-WT, **b** HIV-1/PrP-Δ24-28 cells, **c** HIV-1/PrP-ΔGPI and **d** HIV-1/PrP-ΔHC cells. *Right panel* is a 2.6 magnification of the selected region (*white box* in the *medium panel*). *Scale bar* is 15 μm

mutant has no significant effect. Interestingly, quantification of cytoplasmic viral mRNAs by quantitative RT-PCR revealed that FL-PrP^C, like PrP^{C}Δ24-28, had no significant effect on the amount of viral RNA compared to the GFP control (middle panel), indicating that PrP^C negatively modulates the translational rate of HIV-1 as judged by the ratio of Renilla activity/cytoplasmic viral genomic RNA (see right panel). To determine if the effect of PrP^C on viral genomic RNA translation is specific to HIV-1, similar experiments were carried out using a construct encoding the *renilla* gene under the control of the CMV promoter with the 5′UTR region of the *beta-globin* gene (Fig. 7d). Under these conditions, we found that FL-PrP^C expression had no impact on the renilla activity (left panel) or the cytoplasmic RNAs (middle panel) and, as a consequence, had no effect on the translational rate of the *renilla*-encoding gene (right panel). These data thus suggest that PrP^C binds to the HIV-1 RNA genome and specifically affects its translation.

Distribution of PrP^C and PrP-mutants in 293T HIV-1 coexpressing cells

To investigate whether PrP^C anti-viral properties can be linked to the PrP^C cellular distribution, immunofluorescence experiments using PrP SAF32 antibody were carried out on 293T HIV-1/PrP-WT or HIV-1/PrP-mutant (ΔGPI, ΔHC, Δ24-28) coexpressing cells. The data presented in Fig. 8 indicated that PrP^C displays as expected a binary distribution, i.e., at the plasma membrane, but also in the cytoplasm, whereas PrP-ΔGPI was only recovered in the cytosol, confirming previous published results [46]. Contrarily, we also found that deletion of the amino terminal polybasic domain (PrP-Δ24-28) enhances the localization of PrP to the PM, confirming previously published results [47], which indicated that this domain is important for PrP endocytosis. Analysis of the 293T HIV-1/PrP-ΔHC indicated that this mutant is also well enriched at the PM, thus suggesting that membrane association is important for the anti-viral properties of PrP.

Shortly before or after its localization to the cell surface, PrP^C is submitted to different endoproteolytic cleavages (Fig. S8A; [6]). The first cleavage, termed α-cleavage, generates the N1/C1 fragments (9–11 kDa/16–18 kDa) and is due to enzymes from the ADAM superfamily (A Disintegrin And Metalloprotease such as ADAM 10 and 17). The second cleavage, termed β-cleavage, generates the N2/C2 fragments (7–8 kDa/20–21 kDa) and is induced by the reactive oxygen species (ROS) without the need for enzymes. To determine whether these cleavages can play a role in the anti-viral properties of PrP^C, protein extracts from 293T HIV-1/PrP^C-WT or mutants (ΔGPI, ΔHC, Δ24-28 or Δ24-245) were treated by the PNGase F enzyme for deglycosylation, and analyzed by Western blotting using the amino terminal or carboxy-terminal SAF32 and SFA70 antibodies, respectively (Fig. S8A). The data presented in Fig. S8B indicate the presence of the C1 fragment (16–18 kDa) in samples HIV-1/PrP^C-WT (lane 4), HIV-1/PrP-ΔHC (lane 8) and HIV-1/PrP-Δ24-28 (lane 10). Since PrP-Δ24-28 has no effect on HIV-1 expression, production and infectivity, we can conclude that α-cleavage, although not present in all samples, is not crucial for the PrP^C anti-viral properties. Similar results were also obtained in the absence of HIV-1, suggesting that HIV-1 expression does not initiate and/or modulate such a cleavage (data not shown).

Discussion

PrP^C is highly conserved among species and is involved in different important cellular processes in vitro and in vivo. In the last decade, a number of reports have indicated that PrP^C can inhibit the replication of different viruses, suggesting that it could act as a host cellular defense factor. In this study, we have extended our knowledge on the anti-HIV-1 properties of PrP^C. We demonstrated that PrP^C strongly affects HIV-1 Gag expression and virus production, and we have identified a small basic domain, 24-KRPKP-28, located in the unstructured N-terminal part of PrP^C as a major determinant of this inhibition. Moreover, we report, for the first time, that PrP^C binds to the viral genomic RNA in cell culture and negatively affects the translation of the HIV-1 Gag polyprotein. These results explain why PrP^C expression strongly affected HIV-1 expression and virus production in our 293T cellular system. In addition, in infected T cells, a more relevant cellular system, we found that PrP^C colocalizes with HIV-1 Gag and Env at the plasma membrane and especially at the virological synapse during cell–cell contact. In infected T cells, we found that PrP^C is strongly released into the extracellular medium during infection and is associated with viral particles. In the course of our study, we observed that cells highly positive for PrP^C express lower levels of HIV-1 Env and Gag, and vice versa, confirming the effect observed in our 293T cell system. In agreement with this inverse correlation, we found that depletion of PrP^C in infected T cells and infected microglial cells stimulates HIV-1 replication, confirming its negative impact on the HIV-1 life cycle. In addition, we also found that virions produced by KD-PrP^C cells are more infectious compared to virions released by KD-Lu negative control cells. These data correlated well with those found in the 293T cell system where virus infectivity was reduced when PrP^C-wt or PrP^C-ΔHC was overexpressed. A comparison of PrP^C with the restriction factor Tetherin revealed that PrP^C inhibits HIV-1 by a different mechanism, but our data

revealed that coexpression of PrP^C and Tetherin induces a strong additive and negative effect on HIV-1 expression and virus production. In light of the wild and strong expression of this protein in cells of the nervous and immune systems, both natural targets of HIV-1 replication in vivo, these data suggest that PrP^C could be a modulator factor of HIV-1 replication.

While most studies failed to demonstrate any secondary structure for the flexible N-terminal part of PrP^C, many investigations have revealed that this region can mediate several biological functions and can bind ligands such as glycosaminoglycans, heparan sulfate, the stress inducible protein 1 (STI-1) as well as copper (for a review, see [1]). We show that PrP^C anti-HIV-1 properties are tightly associated with a small basic domain, 24-KRPKP-28, located in the N-terminal part of the protein. Interestingly, this small basic domain is part of the binding regions of negatively charged molecules such as glycosaminoglycan or heparan sulfate, suggesting that this domain could be part of an RNA-binding domain. Other activities, such as PrP^C internalization, were also found to be associated with this small basic domain [47] or, as recently published, with antimicrobial activity [48], thus confirming the importance of this region in PrP^C-associated cellular processes. Because the $PrP^C\Delta$23-145 mutant affects HIV-1 expression and virus production with less efficiency than the $PrP^C\Delta$24-28 mutant, we selected other potential domains containing basic residues and tested whether their deletion could also reverse or block the negative effect of WT PrP^C. Using these mutants, we failed to identify secondary domains that could be directly involved with the restrictive effect of PrP^C. However, we cannot exclude that such domains, in combination, could be involved as secondary helper domains.

The transmembrane/hydrophobic core (TM/HC) domain (residues 112–130) is essential for the ^{CTM}PrP isoform formation. Surprisingly, we found that the TM/HC domain deletion mutant acts as a dominant negative form of PrP^C, affecting both HIV-1 expression and production even more severely than WT PrP^C. Interestingly, a recent study revealed that neuronal protein synthesis is enhanced when the stress-inducible protein 1 (STI-1) binds the PrP^C HC/TM domain (residues 113–128) [49, 50], and this interaction facilitates the anti-oxidative stress activity of PrP^C [51]. HIV-1 Tat, Env and Vpr proteins all stimulate oxidative stress [52–56], which can be beneficial for HIV-1 replication [57]. Indeed, it was recently shown that the HIV-1 internal ribosome entry site (IRES) that controls the expression of viral Gag structural proteins was strongly stimulated during the induction of oxidative stress [57]. PrP^C has anti-oxidative stress properties that are well characterized (for reviews, see [1, 6]). We hypothesize that PrP^C could counteract the positive effects of oxidative stress on HIV-1 Gag translation. This hypothesis is currently under investigation.

Despite the clear negative impact of PrP^C expression on the replication of different viruses such as MuLV, HIV-1 and adenovirus-5, the molecular basis of this inhibition remains uncharacterized. Most PrP^C ($\sim$90%) molecules are exposed to the outer surface of the cell membrane. Less than 10% of PrP^C molecules are also associated with membranes as a transmembrane ^{CTM}PrP isoform (the N-terminus being exposed in the cytosol) or recovered in the cytosoplasm as a cytosolic PrP isoform (cytPrP) [39]. In this report, we conclude that the ^{CTM}PrP isoform is not directly involved in the inhibition of HIV-1. Interestingly, the cytPrP isoform was recently discovered to be involved in aggresome formation and was found, when overexpressed, to strongly inhibit general protein synthesis [58, 59]. Because HIV-1 Gag is translated in the cytoplasm, cytPrP would theoretically be a good candidate that could easily bind the viral genomic RNA and inhibit HIV-1 Gag translation. However, our data also indicated that, under our experimental conditions, general protein synthesis was not affected. These data suggest that the mechanism involved in the Gag decrease is different from that previously published for cytPrP [58]. We do not know whether HIV-1 expression could enhance cytPrP formation, but we cannot exclude that such a form of PrP could be generated and participate to these antiviral properties.

In 2004, we previously found that PrP-ΔGPI has only a minor effect on HIV-1 expression and production compared to PrP^C-WT [25]. Here we also confirmed these data, indicating that anchoring PrP^C to the membrane is essential for the anti-viral properties. Only a few studies specifically characterized the properties of PrP-ΔGPI in a non-prion disease context. Campana and colleagues [47] found that this mutant is tethered to the cell membranes and associates to membrane DRMs. However, PrP-ΔGPI was not distributed at the cell surface but in the cytosol and was mainly released in the culture media. In our 293T cellular model we also found that PrP-ΔGPI is associated with DRMs (data not shown), and immunofluorescence experiments realized on 293T HIV-1/PrP coexpressing cells confirmed that PrP-ΔGPI is not distributed on the PM but is localized in the cytosol (see Fig. 8). These data suggest that physical association of PrP^C to the PM can be a crucial feature for the anti-viral properties. However, by IF, we also found that PrPΔ24-28, which remains almost entirely associated to the PM (it was also associated to raft microdomains; [47]), has only a moderate negative effect on HIV-1. Because the 24–28 residues have been shown to be involved in the endocytosis process and in the binding to RNAs, it is difficult in this case to determine whether association to the PM is essential. However, we found by IF that PrP-ΔHC mutant, which strongly affects HIV-1

production and expression, is enriched at the PM, suggesting that membrane association and presence of the polybasic region are important for the anti-viral properties. The lack of the GPI anchor clearly modifies the trafficking pathway of the protein. In this context we can hypothesize that access to the viral genomic RNA could be compromised in spite of the presence of the polybasic region.

Many studies have indicated that PrP^C can bind different sources of RNAs [60–63]. Among them, it was shown that PrP efficiently binds some highly structured RNAs [60–63]. In vitro, we previously found that recombinant PrP^C efficiently binds the highly structured HIV-1 TAR sequence located in the 5′ untranslated region (5′ UTR) of viral mRNAs and that PrP-TAR binding generates high nucleoprotein complexes [22, 23]. Interestingly, Weiss et al. [63] found that residues 23–52 were essential for the binding to structured RNA aptamers, which correlates well with the data we obtained with the PrPΔ24-28 mutant in our translation experiments. Here we found in cell culture that viral genomic RNA is associated with PrP^C immunoprecipitates. These data suggest that PrP^C could bind the 5′ UTR and subsequently inhibit mRNA translation. Interestingly, the TAR sequence is also present in the subgenomic RNA encoding the envelope glycoprotein. Here, we confirmed that Env-SUgp120 expression was strongly reduced in PrP^C/HIV-1 coexpressing 293T cells [25]. Using deletion mutants described above, we found that WT-PrP^C and PrP-ΔHC/TM strongly inhibit Env-SUgp120 expression, whereas PrP-ΔGPI and PrP-Δ24-28 do not (see Fig. S3B). Thus, our data suggest that PrP^C could preferentially bind the 5′ UTR of HIV-1 and therefore would negatively modulate the translation of these mRNAs. The mechanism by which PrP^C negatively affects HIV-1 translation is uncharacterized at the present time, but different studies demonstrated that PrP^C, when associated with RNAs, induces the formation of nucleoprotein complexes [60, 61, 64, 65] containing a proteinase K (PK)-resistant misfolded PrP isoform resembling PrP^{Sc} involved in prion diseases. Interestingly, we previously found that a population of PrP molecules in 293T HIV-1/PrP^C expressing cells is partially PK resistant [25]. Additionally, in scrapie-infected cells we found PrP^{Sc} associated with endogenous retroviral RNAs and Gag proteins [66, 67]. In this context, we can hypothesize that translation of HIV-1 RNAs could be inhibited at the level of these PrP nucleoprotein complexes. The nucleoprotein complexes containing the viral RNAs could block the access to the translation machinery.

In the course of our study, we confirmed that Env-SUgp120 expression was strongly decreased when PrP^C-WT and PrP-ΔHC were expressed and as a consequence that virions released in these context were less infectious. Conversely, analyses of virions released by KD-PrP CEM-GFP cells indicated that the decrease of PrP^C expression strongly enhances the virus infectivity, confirming our data on the 293T cell system. Despite the strong impact of PrP^C depletion on HIV-1 infectivity released by KD-PrP cells, the global effect of PrP silencing on the HIV-1 kinetic of infection appears moderated (twofold effect), suggesting that another parameter was modulated. PrP^C was previously found to be involved in the cytoskeleton dynamic and especially by stimulating the formation of filopodia [8] and nanotubes [7]. PrP^C was also found to be a partner of actin and tubulin [68]. In addition, PrP^C was also associated with immunological synapse (IS), and we show here that PrP^C is enriched at the virological synapse (VS). Interestingly, HIV was found to highjack filopodia [69] or TNT communication [70] to spread through an intercellular route between cells or by cell–cell contacts through the virological synapses [44]. Thus, we can suppose that the decrease of PrP^C expression could result in the reduction of these cellular structures (filopodia and nanotubes). According to its cell surface localization, PrP^C was shown to be involved in cell–cell interactions through the binding with homotypic or heterotypic cell surface partners, suggesting that PrP^C could stabilize the virological synapse. In this way, in the PrP^C silencing context, HIV-1 spreading should be negatively affected, explaining at least in part the moderated effect observed in our kinetic experiments. Further studies need to be done to determine whether PrP^C can affect the spreading of HIV-1 by modulating the formation of filopodia or nanotubes or by stabilizing the virological synapse.

Interestingly, in this study we have also reported that Shadoo, but not Doppel, can also affect HIV-1 Gag expression and virus production. Like PrP^C, Shadoo protects cells against physiological stressors. Recent studies have indicated that the N-terminal domain is responsible for this function and that this function maps to the N-terminal domain that can functionally replace that of PrP^C. This suggests that the N-terminus of PrP^C and Shadoo possesses a conserved physiological activity. Recently, published data have revealed that the Shadoo N-terminal domain (and especially the RGG-box region) can also bind nucleic acids, especially RNAs (Lau and Westaway Prion 2010 conference, Salzburg; [71]) suggesting that this domain is most certainly involved in HIV-1 inhibition. The role of Shadoo in the cell defense against viral injury should be investigated in the future.

Recently, Lotscher and colleagues [16] reported that activation of endogeneous murine retroviruses (MuLV/IMERV1) in the germinal centers of mouse spleen following immune stimulation leads to an upregulation of PrP^C expression, which in turn reduces the level of retroviral activity [16]. Using $PrP^{-/-}$ knock-out mice, the inhibition of the MuLV/IMERV1 retroviruses was completely abolished, suggesting that PrP^C silencing must be

total to efficiently block the restriction activity. In agreement with these data, we also confirmed in our cellular system that PrP^C expression affects MoMuLV virus production (Leblanc unpublished data). Similar data were reported for the adenovirus 5, suggesting that this function can be extended to other virus families. The mechanisms involved in this inhibition have not yet been characterized, but interestingly, PrP^C mRNA has also been found to be upregulated not only in hepatocytes 72 h after HCV infection, but also in HIV-1-infected astrocytes [19, 20]. Recently, Roberts et al. [21] observed that PrP^C protein is significantly increased in the CNS of HIV-1-infected individuals with neurocognitive impairment and in SIV-infected macaques with encephalitis [21]. In addition to PrP^C upregulation, it was recently shown that a number of endoplasmic stress-associated proteins were also upregulated in the brain of HIV-infected patients, indicating that HIV infection induces ER stress in the brain [72]. Interestingly, it was recently shown that endoplasmic stress favors the accumulation of cytPrP [73–75]. These data underline the need to better characterize the PrP^C isoforms expressed in the brains of HIV-1-infected patients and to determine whether its upregulation and/or processing could be a potential way to modulate HIV-1 replication in the brain.

The capacity of PrP^C to be associated with cellular membranes but also to be recovered into the cytosol, to bind RNAs and to display nucleic acid chaperone activity, to undergo isoform transition into novel structural conformations and to assemble into nucleopoptein complexes is reminiscent of the cellular and biochemical features of viral proteins such as retroviral Gag polyproteins. We can thus hypothesize that PrP^C anti-HIV-1 activities could be mediated through these virus-like properties.

Acknowledgments We thank Ramanujan Hegde, David Harris, Paul Bieniasz, David Westaway, Jeremy Luban, Serge Bénichou, Didier Trono and Hybridolab for kindly providing biological materials. We thank Olivier Schwartz, Clarisse Berlioz-Torrent and Renaud Mahieux for materials, discussions and help. We thank Robin Buckland and Jenny T. Miller for carefully reading the manuscript. We acknowledge the PLATIM microscope platform at ENS Lyon (SFR Biosciences Gerland–Lyon Sud UMS34444/US8, France). This work was supported by the CNRS, INSERM and GIS-Prion. RSR and TO received grant support from ANRS and Conycit. We thank the ANR program EXOPRION (to PL and GR) for its essential contribution to the definitive version of this work.

References

1. Linden R, Martins VR, Prado MA, Cammarota M, Izquierdo I, Brentani RR (2008) Physiology of the prion protein. Physiol Rev 88(2):673–728. doi:10.1152/physrev.00007.2007
2. Griffiths RE, Heesom KJ, Anstee DJ (2007) Normal prion protein trafficking in cultured human erythroblasts. Blood 110(13): 4518–4525. doi:10.1182/blood-2007-04-085183
3. Guo M, Huang T, Cui Y, Pan B, Shen A, Sun Y, Yi Y, Wang Y, Xiao G, Sun G (2008) PrPC interacts with tetraspanin-7 through bovine PrP154-182 containing alpha-helix 1. Biochem Biophys Res Commun 365(1):154–157. doi:10.1016/j.bbrc.2007.10.160
4. Prusiner SB (1998) Prions. Proc Natl Acad Sci USA 95(23): 13363–13383
5. Isaacs JD, Jackson GS, Altmann DM (2006) The role of the cellular prion protein in the immune system. Clin Exp Immunol 146(1):1–8. doi:10.1111/j.1365-2249.2006.03194.x
6. Mehrpour M, Codogno P (2010) Prion protein: from physiology to cancer biology. Cancer Lett 290(1):1–23. doi:10.1016/j.canlet.2009.07.009
7. Miyazawa K, Emmerling K, Manuelidis L (2010) Proliferative arrest of neural cells induces prion protein synthesis, nanotube formation, and cell-to-cell contacts. J Cell Biochem 111(1):239–247. doi:10.1002/jcb.22723
8. Schrock Y, Solis GP, Stuermer CA (2009) Regulation of focal adhesion formation and filopodia extension by the cellular prion protein (PrPC). FEBS Lett 583(2):389–393. doi:10.1016/j.febslet.2008.12.038
9. Zhang CC, Steele AD, Lindquist S, Lodish HF (2006) Prion protein is expressed on long-term repopulating hematopoietic stem cells and is important for their self-renewal. Proc Natl Acad Sci USA 103(7):2184–2189. doi:10.1073/pnas.0510577103
10. Mattei V, Garofalo T, Misasi R, Circella A, Manganelli V, Lucania G, Pavan A, Sorice M (2004) Prion protein is a component of the multimolecular signaling complex involved in T cell activation. FEBS Lett 560(1–3):14–18. doi:10.1016/S0014-5793(04)00029-8
11. Spielhaupter C, Schatzl HM (2001) PrPC directly interacts with proteins involved in signaling pathways. J Biol Chem 276(48):44604–44612. doi:10.1074/jbc.M103289200
12. Stuermer CA, Langhorst MF, Wiechers MF, Legler DF, Von Hanwehr SH, Guse AH, Plattner H (2004) PrPc capping in T cells promotes its association with the lipid raft proteins reggie-1 and reggie-2 and leads to signal transduction. FASEB J 18(14):1731–1733. doi:10.1096/fj.04-2150fje
13. Mouillet-Richard S, Ermonval M, Chebassier C, Laplanche JL, Lehmann S, Launay JM, Kellermann O (2000) Signal transduction through prion protein. Science 289(5486):1925–1928
14. Neil S, Bieniasz P (2009) Human immunodeficiency virus, restriction factors, and interferon. J Interferon Cytokine Res 29(9):569–580. doi:10.1089/jir.2009.0077
15. Nakamura Y, Sakudo A, Saeki K, Kaneko T, Matsumoto Y, Toniolo A, Itohara S, Onodera T (2003) Transfection of prion protein gene suppresses coxsackievirus B3 replication in prion protein gene-deficient cells. J Gen Virol 84(Pt 12):3495–3502
16. Lotscher M, Recher M, Lang KS, Navarini A, Hunziker L, Santimaria R, Glatzel M, Schwarz P, Boni J, Zinkernagel RM (2007) Induced prion protein controls immune-activated retroviruses in the mouse spleen. PLoS One 2(11):e1158. doi:10.1371/journal.pone.0001158
17. Nikles D, Bach P, Boller K, Merten CA, Montrasio F, Heppner FL, Aguzzi A, Cichutek K, Kalinke U, Buchholz CJ (2005) Circumventing tolerance to the prion protein (PrP): vaccination with PrP-displaying retrovirus particles induces humoral immune responses against the native form of cellular PrP. J Virol 79(7):4033–4042. doi:10.1128/JVI.79.7.4033-4042.2005
18. Caruso P, Burla R, Piersanti S, Cherubini G, Remoli C, Martina Y, Saggio I (2009) Prion expression is activated by Adenovirus 5 infection and affects the adenoviral cycle in human cells. Virology 385(2):343–350. doi:10.1016/j.virol.2008.12.005
19. Muller WE, Pfeifer K, Forrest J, Rytik PG, Eremin VF, Popov SA, Schroder HC (1992) Accumulation of transcripts coding for prion protein in human astrocytes during infection with human

immunodeficiency virus. Biochim Biophys Acta 1139(1–2):32–40 (0925-4439(92)90079-3)
20. Walters KA, Joyce MA, Thompson JC, Smith MW, Yeh MM, Proll S, Zhu LF, Gao TJ, Kneteman NM, Tyrrell DL, Katze MG (2006) Host-specific response to HCV infection in the chimeric SCID-beige/Alb-uPA mouse model: role of the innate antiviral immune response. PLoS Pathog 2(6):59. doi:10.1371/journal.ppat.0020059
21. Roberts TK, Eugenin EA, Morgello S, Clements JE, Zink MC, Berman JW (2010) PrPC, the cellular isoform of the human prion protein, is a novel biomarker of HIV-associated neurocognitive impairment and mediates neuroinflammation. Am J Pathol 177(4):1848–1860. doi:10.2353/ajpath.2010.091006
22. Gabus C, Auxilien S, Pechoux C, Dormont D, Swietnicki W, Morillas M, Surewicz W, Nandi P, Darlix JL (2001) The prion protein has DNA strand transfer properties similar to retroviral nucleocapsid protein. J Mol Biol 307(4):1011–1021. doi:10.1006/jmbi.2001.4544
23. Gabus C, Derrington E, Leblanc P, Chnaiderman J, Dormont D, Swietnicki W, Morillas M, Surewicz WK, Marc D, Nandi P, Darlix JL (2001) The prion protein has RNA binding and chaperoning properties characteristic of nucleocapsid protein NCP7 of HIV-1. J Biol Chem 276(22):19301–19309. doi:10.1074/jbc.M009754200
24. Moscardini M, Pistello M, Bendinelli M, Ficheux D, Miller JT, Gabus C, Le Grice SF, Surewicz WK, Darlix JL (2002) Functional interactions of nucleocapsid protein of feline immunodeficiency virus and cellular prion protein with the viral RNA. J Mol Biol 318(1):149–159. doi:10.1016/S0022-2836(02)00092-X
25. Leblanc P, Baas D, Darlix JL (2004) Analysis of the interactions between HIV-1 and the cellular prion protein in a human cell line. J Mol Biol 337(4):1035–1051. doi:10.1016/j.jmb.2004.02.007
26. Leblanc P, Alais S, Porto-Carreiro I, Lehmann S, Grassi J, Raposo G, Darlix JL (2006) Retrovirus infection strongly enhances scrapie infectivity release in cell culture. EMBO J 25(12):2674–2685. doi:10.1038/sj.emboj.7601162
27. Adachi A, Gendelman HE, Koenig S, Folks T, Willey R, Rabson A, Martin MA (1986) Production of acquired immunodeficiency syndrome-associated retrovirus in human and nonhuman cells transfected with an infectious molecular clone. J Virol 59(2):284–291
28. Watts JC, Huo H, Bai Y, Ehsani S, Jeon AH, Shi T, Daude N, Lau A, Young R, Xu L, Carlson GA, Williams D, Westaway D, Schmitt-Ulms G (2009) Interactome analyses identify ties of PrP and its mammalian paralogs to oligomannosidic N-glycans and endoplasmic reticulum-derived chaperones. PLoS Pathog 5(10):1000608. doi:10.1371/journal.ppat.1000608
29. Chakrabarti O, Hegde RS (2009) Functional depletion of mahogunin by cytosolically exposed prion protein contributes to neurodegeneration. Cell 137(6):1136–1147. doi:10.1016/j.cell.2009.03.042
30. Rane NS, Chakrabarti O, Feigenbaum L, Hegde RS (2010) Signal sequence insufficiency contributes to neurodegeneration caused by transmembrane prion protein. J Cell Biol 188(4):515–526. doi:10.1083/jcb.200911115
31. Neil SJ, Zang T, Bieniasz PD (2008) Tetherin inhibits retrovirus release and is antagonized by HIV-1 Vpu. Nature 451(7177):425–430. doi:10.1038/nature06553
32. Naldini L, Blomer U, Gallay P, Ory D, Mulligan R, Gage FH, Verma IM, Trono D (1996) In vivo gene delivery and stable transduction of nondividing cells by a lentiviral vector. Science 272(5259):263–267
33. Goujon C, Arfi V, Pertel T, Luban J, Lienard J, Rigal D, Darlix JL, Cimarelli A (2008) Characterization of simian immunodeficiency virus SIVSM/human immunodeficiency virus type 2 Vpx function in human myeloid cells. J Virol 82(24):12335–12345. doi:10.1128/JVI.01181-08
34. Hamard-Peron E, Juillard F, Saad JS, Roy C, Roingeard P, Summers MF, Darlix JL, Picart C, Muriaux D (2010) Targeting of murine leukemia virus gag to the plasma membrane is mediated by PI(4, 5)P2/PS and a polybasic region in the matrix. J Virol 84(1):503–515. doi:10.1128/JVI.01134-09
35. Ricci EP, Herbreteau CH, Decimo D, Schaupp A, Datta SA, Rein A, Darlix JL, Ohlmann T (2008) In vitro expression of the HIV-2 genomic RNA is controlled by three distinct internal ribosome entry segments that are regulated by the HIV protease and the Gag polyprotein. RNA 14(7):1443–1455. doi:10.1261/rna.813608
36. Watts JC, Westaway D (2007) The prion protein family: diversity, rivalry, and dysfunction. Biochim Biophys Acta 1772(6):654–672. doi:10.1016/j.bbadis.2007.05.001
37. Young R, Passet B, Vilotte M, Cribiu EP, Beringue V, Le Provost F, Laude H, Vilotte JL (2009) The prion or the related Shadoo protein is required for early mouse embryogenesis. FEBS Lett 583(19):3296–3300. doi:10.1016/j.febslet.2009.09.027
38. Van Damme N, Goff D, Katsura C, Jorgenson RL, Mitchell R, Johnson MC, Stephens EB, Guatelli J (2008) The interferon-induced protein BST-2 restricts HIV-1 release and is downregulated from the cell surface by the viral Vpu protein. Cell Host Microbe 3(4):245–252. doi:10.1016/j.chom.2008.03.001
39. Chakrabarti O, Ashok A, Hegde RS (2009) Prion protein biosynthesis and its emerging role in neurodegeneration. Trends Biochem Sci 34(6):287–295. doi:10.1016/j.tibs.2009.03.001
40. Kupzig S, Korolchuk V, Rollason R, Sugden A, Wilde A, Banting G (2003) Bst-2/HM1.24 is a raft-associated apical membrane protein with an unusual topology. Traffic 4(10):694–709 (129)
41. Perez-Caballero D, Zang T, Ebrahimi A, McNatt MW, Gregory DA, Johnson MC, Bieniasz PD (2009) Tetherin inhibits HIV-1 release by directly tethering virions to cells. Cell 139(3):499–511. doi:10.1016/j.cell.2009.08.039
42. Gousset K, Schiff E, Langevin C, Marijanovic Z, Caputo A, Browman DT, Chenouard N, de Chaumont F, Martino A, Enninga J, Olivo-Marin JC, Mannel D, Zurzolo C (2009) Prions hijack tunnelling nanotubes for intercellular spread. Nat Cell Biol 11(3):328–336. doi:10.1038/ncb1841
43. Ballerini C, Gourdain P, Bachy V, Blanchard N, Levavasseur E, Gregoire S, Fontes P, Aucouturier P, Hivroz C, Carnaud C (2006) Functional implication of cellular prion protein in antigen-driven interactions between T cells and dendritic cells. J Immunol 176(12):7254–7262 (176/12/7254)
44. Rudnicka D, Feldmann J, Porrot F, Wietgrefe S, Guadagnini S, Prevost MC, Estaquier J, Haase AT, Sol-Foulon N, Schwartz O (2009) Simultaneous cell-to-cell transmission of human immunodeficiency virus to multiple targets through polysynapses. J Virol 83(12):6234–6246. doi:10.1128/JVI.00282-09
45. Sourisseau M, Sol-Foulon N, Porrot F, Blanchet F, Schwartz O (2007) Inefficient human immunodeficiency virus replication in mobile lymphocytes. J Virol 81(2):1000–1012. doi:10.1128/JVI.01629-06
46. Campana V, Caputo A, Sarnataro D, Paladino S, Tivodar S, Zurzolo C (2007) Characterization of the properties and trafficking of an anchorless form of the prion protein. J Biol Chem 282(31):22747–22756. doi:10.1074/jbc.M701468200
47. Sunyach C, Jen A, Deng J, Fitzgerald KT, Frobert Y, Grassi J, McCaffrey MW, Morris R (2003) The mechanism of internalization of glycosylphosphatidylinositol-anchored prion protein. EMBO J 22(14):3591–3601. doi:10.1093/emboj/cdg344
48. Pasupuleti M, Roupe M, Rydengard V, Surewicz K, Surewicz WK, Chalupka A, Malmsten M, Sorensen OE, Schmidtchen A (2009) Antimicrobial activity of human prion protein is mediated by its N-terminal region. PLoS One 4(10):e7358. doi:10.1371/journal.pone.0007358
49. Zanata SM, Lopes MH, Mercadante AF, Hajj GN, Chiarini LB, Nomizo R, Freitas AR, Cabral AL, Lee KS, Juliano MA, de

Oliveira E, Jachieri SG, Burlingame A, Huang L, Linden R, Brentani RR, Martins VR (2002) Stress-inducible protein 1 is a cell surface ligand for cellular prion that triggers neuroprotection. EMBO J 21(13):3307–3316. doi:10.1093/emboj/cdf325

50. Roffe M, Beraldo FH, Bester R, Nunziante M, Bach C, Mancini G, Gilch S, Vorberg I, Castilho BA, Martins VR, Hajj GN (2010) Prion protein interaction with stress-inducible protein 1 enhances neuronal protein synthesis via mTOR. Proc Natl Acad Sci USA 107(29):13147–13152. doi:10.1073/pnas.1000784107
51. Sakudo A, Lee DC, Nishimura T, Li S, Tsuji S, Nakamura T, Matsumoto Y, Saeki K, Itohara S, Ikuta K, Onodera T (2005) Octapeptide repeat region and N-terminal half of hydrophobic region of prion protein (PrP) mediate PrP-dependent activation of superoxide dismutase. Biochem Biophys Res Commun 326(3): 600–606. doi:10.1016/j.bbrc.2004.11.092
52. Deshmane SL, Mukerjee R, Fan S, Del Valle L, Michiels C, Sweet T, Rom I, Khalili K, Rappaport J, Amini S, Sawaya BE (2009) Activation of the oxidative stress pathway by HIV-1 Vpr leads to induction of hypoxia-inducible factor 1alpha expression. J Biol Chem 284(17):11364–11373. doi:10.1074/jbc.M809266200
53. Nicolini A, Ajmone-Cat MA, Bernardo A, Levi G, Minghetti L (2001) Human immunodeficiency virus type-1 Tat protein induces nuclear factor (NF)-kappaB activation and oxidative stress in microglial cultures by independent mechanisms. J Neurochem 79(3):713–716
54. Pocernich CB, Sultana R, Mohmmad-Abdul H, Nath A, Butterfield DA (2005) HIV-dementia, Tat-induced oxidative stress, and antioxidant therapeutic considerations. Brain Res Brain Res Rev 50(1):14–26. doi:10.1016/j.brainresrev.2005.04.002
55. Price TO, Ercal N, Nakaoke R, Banks WA (2005) HIV-1 viral proteins gp120 and Tat induce oxidative stress in brain endothelial cells. Brain Res 1045(1–2):57–63. doi:10.1016/j.brainres.2005.03.031
56. Ronaldson PT, Bendayan R (2008) HIV-1 viral envelope glycoprotein gp120 produces oxidative stress and regulates the functional expression of multidrug resistance protein-1 (Mrp1) in glial cells. J Neurochem 106(3):1298–1313. doi:10.1111/j.1471-4159.2008.05479.x
57. Gendron K, Ferbeyre G, Heveker N, Brakier-Gingras L (2011) The activity of the HIV-1 IRES is stimulated by oxidative stress and controlled by a negative regulatory element. Nucleic Acids Res 39(3):902–912. doi:10.1093/nar/gkq885
58. Goggin K, Beaudoin S, Grenier C, Brown AA, Roucou X (2008) Prion protein aggresomes are poly(A)+ ribonucleoprotein complexes that induce a PKR-mediated deficient cell stress response. Biochim Biophys Acta 1783(3):479–491. doi:10.1016/j.bbamcr.2007.10.008
59. Grenier C, Bissonnette C, Volkov L, Roucou X (2006) Molecular morphology and toxicity of cytoplasmic prion protein aggregates in neuronal and non-neuronal cells. J Neurochem 97(5):1456–1466. doi:10.1111/j.1471-4159.2006.03837.x
60. Adler V, Zeiler B, Kryukov V, Kascsak R, Rubenstein R, Grossman A (2003) Small, highly structured RNAs participate in the conversion of human recombinant PrP(Sen) to PrP(Res) in vitro. J Mol Biol 332(1):47–57 (S0022283603009197)
61. Deleault NR, Lucassen RW, Supattapone S (2003) RNA molecules stimulate prion protein conversion. Nature 425(6959):717–720. doi:10.1038/nature01979
62. Gomes MP, Cordeiro Y, Silva JL (2008) The peculiar interaction between mammalian prion protein and RNA. Prion 2(2):64–66 (6988)
63. Weiss S, Proske D, Neumann M, Groschup MH, Kretzschmar HA, Famulok M, Winnacker EL (1997) RNA aptamers specifically interact with the prion protein PrP. J Virol 71(11):8790–8797
64. Nandi PK, Leclerc E (1999) Polymerization of murine recombinant prion protein in nucleic acid solution. Arch Virol 144(9): 1751–1763 (91441751.705)
65. Nandi PK, Nicole JC (2004) Nucleic acid and prion protein interaction produces spherical amyloids which can function in vivo as coats of spongiform encephalopathy agent. J Mol Biol 344(3):827–837. doi:10.1016/j.jmb.2004.09.080
66. Alais S, Simoes S, Baas D, Lehmann S, Raposo G, Darlix JL, Leblanc P (2008) Mouse neuroblastoma cells release prion infectivity associated with exosomal vesicles. Biol Cell 100(10): 603–615. doi:10.1042/BC20080025
67. Manuelidis L (2007) A 25 nm virion is the likely cause of transmissible spongiform encephalopathies. J Cell Biochem 100(4):897–915. doi:10.1002/jcb.21090
68. Zafar S, von Ahsen N, Oellerich M, Zerr I, Schulz-Schaeffer WJ, Armstrong VW, Asif AR (2011) Proteomics approach to identify the interacting partners of cellular prion protein and characterization of Rab7a interaction in neuronal cells. J Proteome Res 10(7):3123–3135. doi:10.1021/pr2001989
69. Sherer NM, Lehmann MJ, Jimenez-Soto LF, Horensavitz C, Pypaert M, Mothes W (2007) Retroviruses can establish filopodial bridges for efficient cell-to-cell transmission. Nat Cell Biol 9(3):310–315. doi:10.1038/ncb1544
70. Eugenin EA, Gaskill PJ, Berman JW (2009) Tunneling nanotubes (TNT) are induced by HIV-infection of macrophages: a potential mechanism for intercellular HIV trafficking. Cell Immunol 254(2):142–148. doi:10.1016/j.cellimm.2008.08.005
71. Corley SM, Gready JE (2008) Identification of the RGG box motif in Shadoo: RNA-binding and signaling roles? Bioinform Biol Insights 2:383–400
72. Lindl KA, Akay C, Wang Y, White MG, Jordan-Sciutto KL (2007) Expression of the endoplasmic reticulum stress response marker, BiP, in the central nervous system of HIV-positive individuals. Neuropathol Appl Neurobiol 33(6):658–669. doi:10.1111/j.1365-2990.2007.00866.x
73. Kang SW, Rane NS, Kim SJ, Garrison JL, Taunton J, Hegde RS (2006) Substrate-specific translocational attenuation during ER stress defines a pre-emptive quality control pathway. Cell 127(5):999–1013. doi:10.1016/j.cell.2006.10.032
74. Orsi A, Fioriti L, Chiesa R, Sitia R (2006) Conditions of endoplasmic reticulum stress favor the accumulation of cytosolic prion protein. J Biol Chem 281(41):30431–30438. doi:10.1074/jbc.M605320200
75. Rane NS, Kang SW, Chakrabarti O, Feigenbaum L, Hegde RS (2008) Reduced translocation of nascent prion protein during ER stress contributes to neurodegeneration. Dev Cell 15(3):359–370. doi:10.1016/j.devcel.2008.06.015